BERICHTE

aus dem Fachbereich Geowissenschaften der Universität Bremen

No. 164

Devey, C.W. , Z. Bond, R. Dunk, J. Gharib, G. Junge, K. Lackschewitz, C. Lear, M. Mottl, J. Pracht, M. Rudnicki, C. Scholz, B. Schramm, S. Severmann, G. Wheat

REPORT AND PRELIMINARY RESULTS OF SONNE CRUISE SO 145/2, TALCAHUANO (CHILE) - ARICA (CHILE), FEBRUARY 4 - FEBRUARY 29, 2000.

Berichte, Fachbereich Geowissenschaften, Universität Bremen, No. 164
63 pages, Bremen 2000

ISSN 0931-0800

The "Berichte aus dem Fachbereich Geowissenschaften" are produced at irregular intervals by the Department of Geosciences, Bremen University.

They serve for the publication of experimental works, Ph.D.-theses and scientific contributions made by members of the department.

Reports can be ordered from:

Gisela Boelen

Sonderforschungsbereich 261

Universität Bremen

Postfach 330 440

D 28334 BREMEN

Phone: (49) 421 218-4124

Fax: (49) 421 218-3116

e-mail: boelen@uni-bremen.de

Citation:

Devey, C. and cruise participants

Report and preliminiary results of Sonne Cruise SO 145/2, Talcahuano (Chile) - Arica (Chile), February 4 – February 29, 2000.

Berichte, Fachbereich Geowissenschaften, Universität Bremen, No. 164, 63 pages, Bremen, 2000.

ISSN 0931-0800

Cruise Report

SO 145/2

EXCO II Leg 2

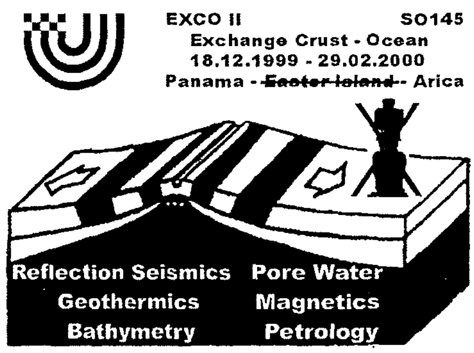

Talcahuano – Arica
4.2.00 – 29.2.00

Alphabetical list of cruise participants

Zoe Bond	SOC
Prof. Dr. Colin W. Devey	UniHB
Rachel Dunk	SOC
Jamshid Gharib	UHaw
Grit Junge	BEO
Dr. Klas Lackschewitz	UniHB
Caroline Lear	UCamb
Dr. Mike Mottl	UHaw
Jens Pracht	UHeid
Dr. Mark Rudnicki	UCamb
Christian Scholz	UHeid
Burkhard Schramm	UniHB
Silke Severmann	SOC
Dr. Geoff Wheat	UAI

UniHB – Fachbereich 5 – Geowissenschaften, Klagenfurterstr. D-28334 Bremen, Germany
BEO - Forschungszentrum Jülich, Aussenstelle BEO Warnemünde, D-18112 Rostock, Germany
UHeid - Geologisch-Paläontologisches Institut, Universität Heidelberg, Im Neuenheimer Feld 234, D-69120 Heidelberg, Germany
UHaw - Dept. Of Oceanography, University of Hawaii, 1000 Pope Road, Honolulu HI 96822, USA
UAI - University of Alaska, Fairbanks, Alaska, U.S.A.
SOC - School of Ocean and Earth Science, Southampton Oceanography Centre, European Way, Empress Dock, Southhampton SO14 3ZH, England
UCamb – Dept. Of Earth Sciences, University of Cambridge, Downing Street, Cambridge, England.

Table of Contents

Acknowledgements

We wish to thank the following people and organisations for their help with the preparation and execution of this cruise

- Captain Papenhagen, his officers and crew for their exceptionally hard work and dedication which enabled us to accomplish far more than we had hoped for in the drastically shortened cruise programme and who made working and living on board a thoroughly enjoyable experience.
- Prof. Dr. Heinrich Villinger and the scientists of cruise SO145/1 for providing us with detailed information on the area which allowed us to plan operations with the maximum of efficieny and success.
- The Bundesministerium für Bildung, Forschung und Technologie (BMBF) and the Projektträger BEO Warnemünde for funding of the cruise and subsequent analytical work.
- The National Science Foundation (NSF, USA) for funding of the participation and subsequent work of Mike Mottl, Geoff Wheat and Jim Gharib
- The Natural Environment Research Council (NERC, UK) for funding the participation and analytical work of the English participants

1. Introduction

1.1Background

The EXCO area (Figure 1.1), a region of „normal" Pacific crust formed at the East Pacific Rise spreading centre around 13°S and well away from extensive influence of major fracture zones or spreading centre jumps, was first studied in 1995 during Sonne cruise SO-105 [*Weigel et al.*, 1996]. These initial studies consisted of seismic, topographic,magnetic and heat flow studies of a strip of seafloor extending from the spreading axis out to 8 million year (Ma) old crust. The aim of these studies was to examine the effects of low-temperature hydrothermal circulation on the aging of the oceanic crust as it drifted away from the active spreading centre. This circulation was thought to be responsible for large changes in the seismic velocities in the upper oceanic crust (Layer 2) between the axis and older crust. This circulation was thought to be controlled strongly by variations in basement topography, with basement lows being regions of water inflow and basement highs concentrating the fluid discharge. The SO-105 results [*Grevemeyer and Weigel*, 1997; *Grevemeyer et al.*, 1998; *Villinger*, 2000] showed a large increase in seismic velocity in Layer 2 away from the axis, and large variations in heat flow density in this area correlating with basement topography, interpreted to be associated with inflow and outflow of circulating pore water.

The EXCO II cruises (SO-145 Legs 1 & 2) were designed to build on this earlier work and explore in more detail the variations in heat flow (Leg 1) and to sample the pore waters and Layer 2 rocks (Leg 2) in an effort to establish the chemical changes which are occurring in this aging crust. A further aim of the rock sampling programme is to examine the variations in magmatic geochemistry of the crust over the last 8 Ma to establish the heterogeneity of magma production and evolution processes through time for a normal spreading segment. It was planned to sample sediments in both low (downflow) and high (upflow) heatflow areas and to dredge at regularly spaced localities to achieve these aims.

1.2 Cruise logisitics

The second leg of the Sonne cruise SO145 was originally planned to leave Easter Island on 28th January 2000 and end in Arica on 29th February 2000. However, due to mechanical problems with the rudder on leg 1, the scientific work had to be prematurely finished and the Sonne was placed in dry dock in Talcahuano, Chile. The dry dock work (7 days) and the extra transit time from Talcahuano to the working area (9 days as against 2 days from Easter Island) meant that the sampling programme on leg 2 had to be drastically reduced, from an originally planned 22 down to 8 working days. It was only possible to make these changes in the sampling programme by omitting several important aspects of the work. It is hoped that these aspects will be studied in a replacement cruise in 2001. A meeting of all cruise participants at the start of the cruise and extensive discussion with Prof. Dr. H. Villinger, Chief Scientist of leg 1, enabled us to assign priorities to the scientific work originally planned and thus we established a modified cruise plan. The emphasis of leg 2 was always on sampling the EXCO region, the modified cruise plan placed the main emphasis on sampling of pore water in sediments in this region, as this pore water sampling is a direct and indispensable complement to the heat flow and

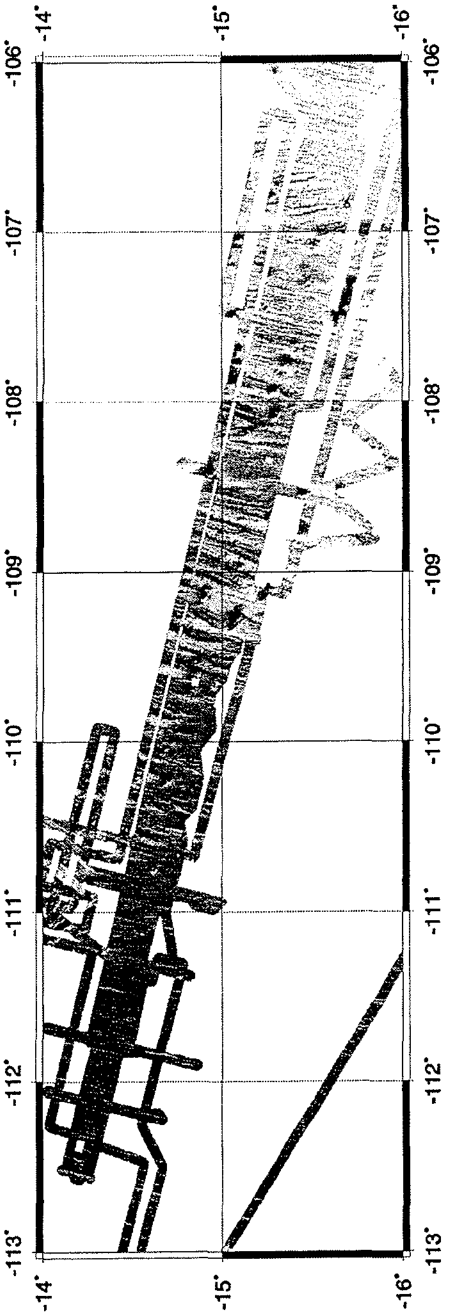

Figure 1.1: Shaded bathymetry of the EXCO area

seismic studies carried out on leg 1. In addition a skeleton sampling of rock samples at various crustal ages was to be performed as preparation for a replacement cruise in 2001.

1.3 Description of the Cruise

The general cruise programme was to make two transects through the study area, starting at 8 Ma crust, sampling up to the spreading axis and then on the return leg concentrating more work on targets identified during the first pass (see cruise track, Figure 1.2). A list of all stations occupied is given in Appendix 1. After nine days transit from Talcahuano, the Sonne arrived in the working area on the morning of 12.2.00 and began sampling sediments on 8 Ma old crust. This area is characterised by heat flow values which are approximately normal for crust of this age and so pore waters collected here were to be used to establish background values. The maximum core recovery was 5m although both 9 and 6m core barrels were deployed. The base of the longest cores was characterised by a highly compacted sediment (see core descriptions, Appendix 2)which appears to have acted as a mechanical barrier prohibiting further penetration of the corer. Also at this position we performed a CTD-station for calibration of the Hydrosweep speed-of-sound-in-water values and collected water samples thoughout the water column for the group from the University of Heidelberg (see Chapters 5&6).

The next series of four sediment stations was on 4 Ma crust in a region where very high heat flow values close to a seamount raised suspicions that a zone of pore water upwelling and discharge may be present. Close to the high heat-flow area was a region with very low heat flow – perhaps the region where pore-water recharge was occurring?

The first successful dredge sampling occurred on 3 Ma crust and yielded altered pillow basalt samples from a steep basement slope. The sampling was guided by maps of slope angle derived from the Hydrosweep bathymetry kindly produced during Leg 1 by Ingo Grevemeyer.

Three cores on 1.5 Ma crust and four cores on 0.3 Ma crust completed the sediment sampling up to the ridge. Despite the relative youth of this crust, core recovery was good – in several cores the presence of rock chips in the core catcher implied that total penetration of the sediment had been achieved and yielded further samples for the rock alteration and magmatic geochemistry studies. One further dredge on 1.2 Ma crust returned empty, a situation which was to be remedied on the return transit.

On the spreading axis itself three dredge stations returned fresh volcanic rock which will be used, together with published data, to establish the along-axis variability of the present magmatic system for comparison with the older rocks. A CTD station provided further water samples for the Heidelberg group and a velocity profile for the ocean at the western-most end of the study area.

For the return leg of the transit, the same crustal ages (0.3, 1.5 and 4 Ma) were selected for more detailed sampling. On-board analyses of the pore water samples (see Chapter 3) collected during the first pass helped identify regions of particular interest and these were then targeted with five core stations each. Dredges at 0.4, 0.75, 2.8, 4.6 and ca. 8 Ma helped to fill in gaps in the sample coverage from the first pass and yielded an overview sampling of the 0-8 Ma age range. Late in the evening of 20.2.00 the last core was brought on board and the return transit to Arica began.

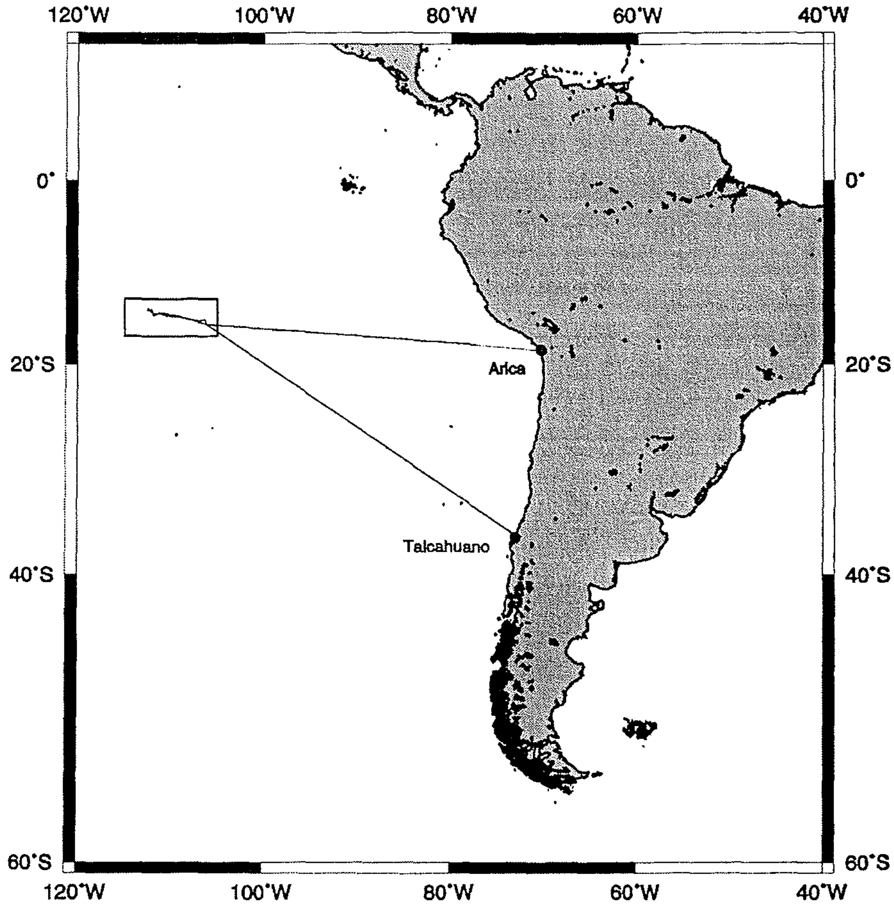

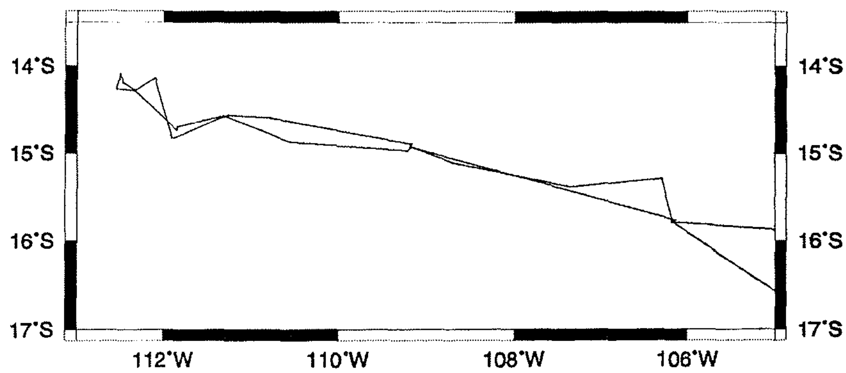

Figure 1.2. Cruise track for SO145/2, overview and details

2. Pore fluid sampling

Zoe Bond, Rachel Dunk, Jim Gharib, Carrie Lear, Mike Mottl, Mark Rudnicki, Silke Severmann, Geoff Wheat

During the EXCO-II cruise, cores brought on deck were sectioned and split according to sampling requirements. Sampling for He isotopic analysis (R. Dunk, Z. Bond) required 10 cm whole sections to be cut at varying lengths along the core; otherwise, the core was sectioned into 1 m lengths. After splitting, each remaining section was halved, described and sampled. Core descriptions were provided by J. Gharib (see Appendix 3). Solid phase samples were taken for porosity determination (SOC), trace element geochemistry (UH, SOC) and foramiferal paleoceanography (UC).

Core descriptions and sample logs are given in the Appendix 3.

Pore fluids were sampled from each split core into centrifuge bottles of 2 different sizes. The smaller size (UH) required approximately 2 cm of undisturbed core section whereas the larger size (SOC) required 5 cm of core section. After chilling to < 5 °C, the small bottles were spun at 21,000 rpm for 4 minutes and the larger bottles for 5,000 rpm for 30 minutes. Centrifuged samples were maintained at < 5 °C prior to filtration and aliquoting. Sample volumes recovered in this way generally totalled ca. 25 ml for each sample depth (2 bottles), with the larger centrifuge bottles yielding roughly double the pore fluid volume of the smaller.

Pore fluid samples were squeezed through Watman 0.45 $_{\mu}$m filters with no pre-filter. Aliquots were taken for shipboard major ion and land based trace element chemistry (M. Mottl, G. Wheat, J. Gharib), $^{87}Sr/^{86}Sr$, $\delta^{6}Li$ and $\delta^{18}O$ analysis (M. Rudnicki), U series isotopes (S. Severmann, R Dunk) and Radium isotopes (G. Henderson, Oxford University).

We would like to thank the watch leaders (C. Devey, K. Lackschewitz, B Schramm) for the efficient provision of core material and the core crew (Luigi Pracht, Christian Scholz) for peerless core handling and cheerfulness in the face of the suprisingly few bent barrels caused during these operations.

3. Pore water chemistry

Geoff Wheat, Mike Mottl, Jim Gharib, Mark Rudnicki, Silke Severmann

Sediment cores were collected as part of EXCO II mainly in order to recover interstitial waters. Despite the shortened Leg we recovered 335 sediment pore water samples from 30 gravity cores, which were taken from four sites with crustal ages of 0.3, 1.5, 4, and 8 Ma. The interstitial water program has two primary objectives:

1) determination of the composition of basement water, over a range of crustal ages and temperatures, in order to assess geochemical fluxes on a young thinly sedimented ridge flank; and
2) determination of patterns and velocities of flow through both the sediments and, by inference, the basement basalt, in order to understand ridge-flank hydrology.

Our strategy, which has proved successful previously on several other ridge flanks, is to target sites for coring that overlie basement highs, and thus have relatively thin sediment and high heat flow. At such sites we have found that water from basement frequently upwells through the sediment column. If this upwelling is sufficiently fast, typically a few mm/y or faster, it allows us to sample basement water which has reacted only minimally with the sediment during its ascent. We also sample sediment over basement troughs with low heat flow, and at intermediate locations, in order to evaluate downwelling and the overall flow pattern within each area, as well as the amount of variation in basement water from one location to another. Whether or not the basement waters are homogenized, for example, tells us a great deal about the amount of seawater flowing through basement and the pathways by which it got there.

On EXCO II we succeeded in sampling several such upwelling areas, but we were also greatly aided by the fact that ten of the 30 cores collected apparently penetrated the entire sediment section: all ten of these cores produced severely dented core cutters and four of them recovered basalt in the core catcher. The youngest site, at 0.3 Ma crustal age, produced six of these cores, while two each came from the 1.5 and 4 Ma sites. These cores to basement give us the best measure of sediment thickness in these three areas and allow us to infer the composition of water in basement even in the absence of upwelling (although several of the cores to basement do show evidence of upwelling).

Pore waters were analyzed at sea for dissolved nitrate, phosphate, fluoride, magnesium, calcium, chlorinity, alkalinity, and pH using standard colorimetric and potentiometric techniques. Analytical precisions are about 1% for nitrate, fluoride, and alkalinity, about 4% for phosphate, and better than 0.5% for magnesium, calcium, and chlorinity. All of these analyses were performed on an 8-ml aliquot of unacidified pore fluid. Results for several of the species are preliminary and will require corrections ashore: nitrate and phosphate for refractive index, and fluoride for extent of complexation with magnesium.

The extensive at-sea analytical program was required to determine whether pore water was flowing and the direction and intensity of this flow. Much of the previous ridge-flank hydrothermal work, mainly on the southern flank of the Costa Rica Rift and the eastern flank of the Juan de Fuca Ridge, has relied on the use of calcium and magnesium to discern the paths and patterns of fluid flow in the crust. In other locations where temperatures in basement are cooler than about 25°C (western flank of the East Pacific Rise and the Mariana Mounds), systematic variations in nitrate profiles have been useful for delineating 1) sources of bottom seawater to basement and 2) areas of venting of pore water and basement fluid to the overlying ocean. Because of the cool crustal conditions in the EXCO corridor, one of the best tracers for fluid flow and circulation is dissolved nitrate (Figures 1 and 2); however, systematic trends in magnesium, calcium, alkalinity, and fluoride also confirm the presence of flow at one of the sites, on 1.5 Ma crust.

Relative to bottom seawater, the concentration of nitrate in pore fluid can either increase as a result of bacterially mediated nitrification, or decrease as a result of bacterially mediated denitrification. Because of variations in sediment type, each of the four sites of different crustal age has a particular rate of reaction for nitrate. A uniform rate within each site is consistent with the close proximity of the cores and the uniformity in sediment type. Thus systematic variations from a "typical" no-flow condition can be used to determine the direction and intensity of flow of the pore water through the sediment column.

On the basis of these flow conditions and the composition of pore waters from the basal sections of those cores with the fastest flow or which penetrated the entire sediment column, we can draw the following preliminary conclusions:

(1) Pore water is upwelling through the sediment column at three of the four sites, at velocities that we will be able to estimate from shore-based modeling, but which appear to be a few millimeters to a few centimeters per year. No flow is evident in any of the five cores from 8 Ma crust.

(2) Upwelling of fluid from basement through the sediment column occurs above basement topographic highs. This finding is consistent with previous work on other, more heavily sedimented ridge flanks; this is the first time, however, that this pattern has been verified on a young flank which has a paucity of sediment and the low basement temperatures inferred from the heat flow data. We found no obvious evidence of downwelling at any of the sites, although additional analysis will be required to confirm this negative finding.

(3) Seawater is flowing through basement on a regional scale in crust that is 1° to 2°C warmer than bottom seawater. These basement temperatures are inferred from thermal gradients of about 0.3°C/m at sites where sediment cores penetrated a sediment column 3 to 56 m thick.

(4) Chlorinity increases slightly at the 0.3 and 8 Ma sites, but the intermediate-age sites have more uniform chlorinity at the value of present-day bottom seawater. At least at the youngest site, the increase is probably due to crustal hydration rather than to the presence of glacial-age seawater in the sediment column. The lack of evidence for hydration at the other sites does not preclude hydration, but rather suggests rapid seawater flow through basement and alteration at a relatively large water-to-rock ratio.

(5) Fluids in basement are young (< 2,000 years old), based on the presence of present-day seawater chlorinity in basal sediment porewaters.

(6) Two distinct fluids reside in basement at the 1.5 (Figure 3) and 4 Ma sites, suggesting a complex pattern of fluid flow and reaction in the crust. One of these fluids has gained magnesium by leaching from basalt and lost calcium, whereas the other has gained calcium and lost magnesium. The latter pattern of Mg uptake into the crust and leaching of calcium is the common one encountered in previous ridge-flank studies, especially at temperatures in excess of 15-25°C. Of the 30 cores from EXCO II, only four show evidence of magnesium uptake into basement.

(7) Alkalinity generally decreases toward basement, consistent with precipitation of calcium carbonate in basement basalt.

(8) Several distinct phosphate-nitrate trends exist. Data from the 4 and 8 Ma sites overlap whereas pore water data from the 1.5 and 0.3 Ma sites do not. Only at the 1.5 Ma site is there more than one general trend in phosphate-nitrate. The general trends are diagnostic of different sediment characteristics among three of the four sites, whereas the different trends at the 1.5 Ma site are consistent with more than one type of fluid in basement.

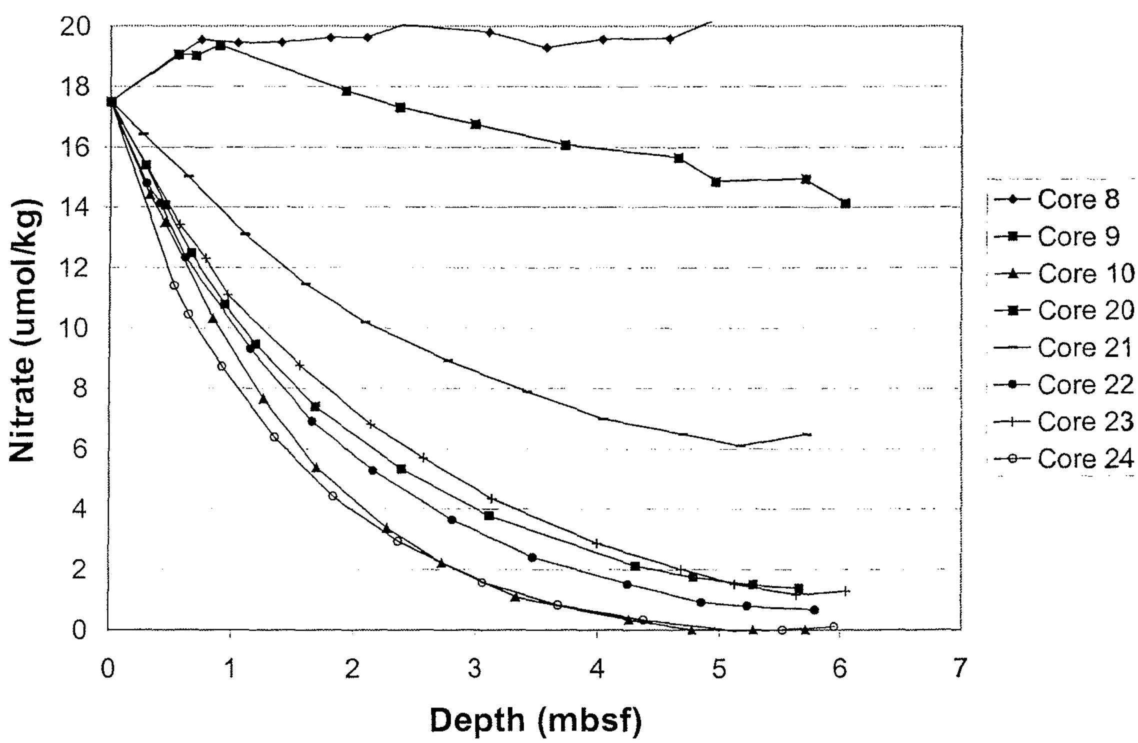

Figure 3.1. Pore water nitrate versus depth from the 1.5 Ma site. Systematic variations in these profiles are consistent with the upwelling of a fluid that has less nitrate than that in bottom seawater. Cores with the fastest pore water upwelling speeds are Cores 10 and 24, which were taken from a topographic and heat flow high. Core 8 was taken in a topographic low which had low heat flow and no evidence for upwelling.

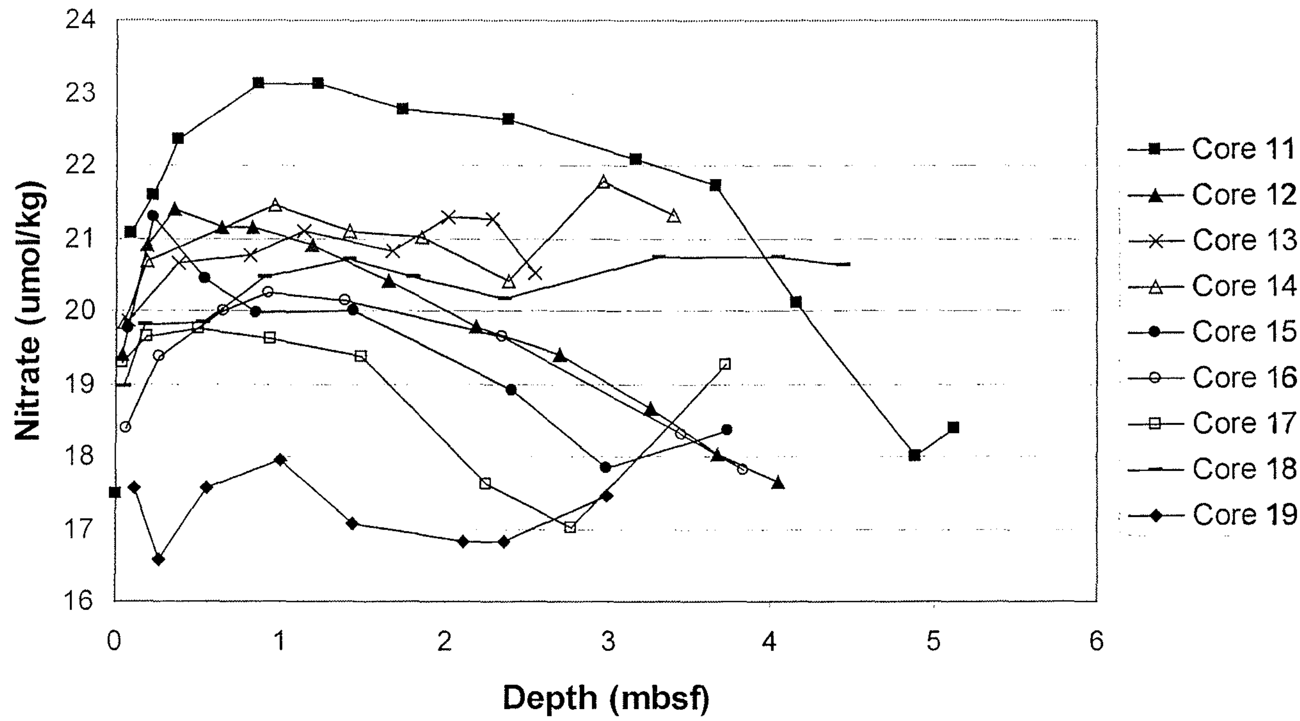

Figure 3.2. Pore water nitrate versus depth from the 0.3 Ma site. Systematic variations in these profiles are consistent with the upwelling of a fluid that has nitrate equal to that in bottom seawater. Core 19 shows the fastest upwelling.

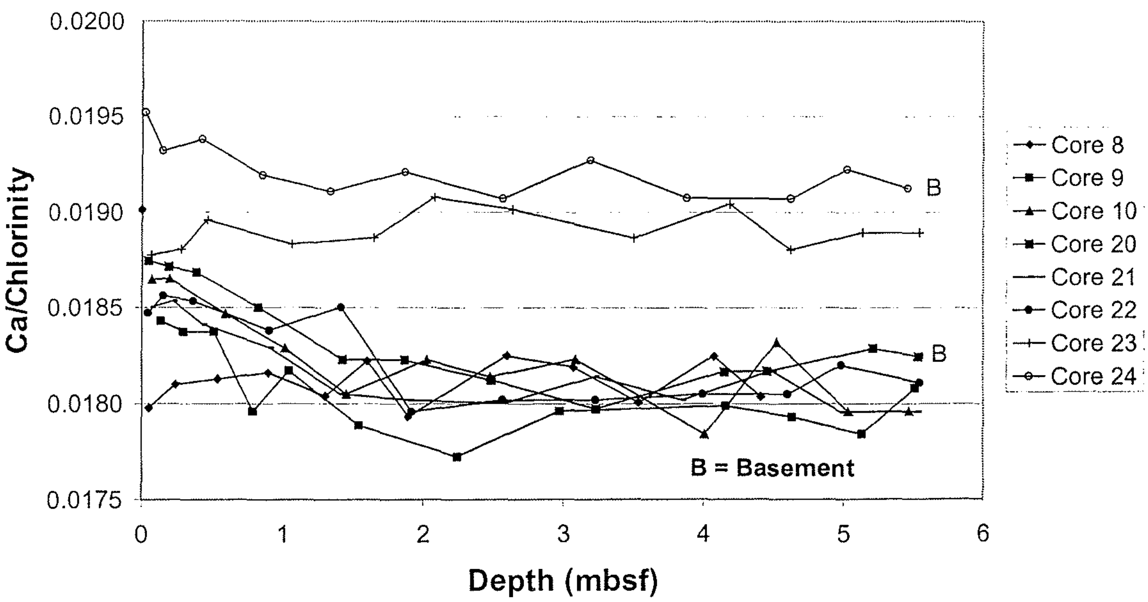

Figure 3.3. Molar ratios of calcium to chlorinity in pore waters from cores from the 1.5 Ma site. The pattern for Mg/chlorinity is opposite to that above. These data support two distinct fluid compositions in basement.

4. Sampling of rocks by dredging

Burkhard Schramm, Colin W. Devey, Grit Junge, Dr. Klas Lackschewitz

During the EXCO II Cruise 145/2 we carried out dredges between the ridge axis at 0.2 Ma and 8.8 Ma [crustal ages and maps taken from Cruise Report 145/1, *Villinger*, 2000] and at two different seamounts on the ridge flanks. Altogether 13 dredges were taken, two of them were empty. A full description of all samples taken from each dredge is given in Appendix 2. The aim of dredging rocks from the seafloor is to study the change in chemistry, the influence of hydrothermal activity and the increase of alteration stage, to investigate the changes in magmatic processes and crustal alteration which have occurred over a time period of ~8.6 Ma. To facilitate dredging and to avoid sediment-cover when dredging, areas with steep basement slopes were chosen as sampling sites.

4.1 Dredge results

Station number	Latitude °S	Longitude °W	Water Depth	Age (Ma)
9 DS	14°52.38	110°32.91	3419	3.0
13 DS	14°43.81	111°51.27	3280	1.3
18 DS	14°15.82	112°32.65	2653	ridge axis at 0.2
20 DS	14°09.23	112°30.90	2648	ridge axis at 0.2
21 DS	14°05.18	112°30.18	2665	ridge axis at 0.2
22 DS	14°11.64	112°27.79	3088	0.4
28 DS	14°08.52	112°06.64	3128	0.75
29 DS	14°49.43	111°54.51	3355	1.4
35 DS	14°35.75	110°45.95	3333	seamount at 2.8
36 DS	14°53.54	109°11.28	3499	4.6
41 DS	15°06.37	108°42.61	3709	seamount at 5.6
42 DS	15°23.05	107°22.01	3873	7.0
43 DS	15°17.58	106°18.13	4118	8.8

Table 4.1: On bottom sampling points of dredges in the working area.

The first dredge in the working area was carried out at 3 Ma (Table 4.1). Collected rocks included aphyric dolerites, basalts and glassy pillows most of them with alteration zoning and weathered glass. Some possess Mn-crusts and rare plagioclase phenocrysts. No rocks were collected by the second dredge. The next 3 dredges were deployed at the ridge axis and included fresh and unaltered basaltic rocks with glass crusts, sheet flows and pillow fragments. Most of them contained rare plagioclase and olivine phenocrysts and some had iron oxide staining, vesicles and Mn-crust. Additionally we found 2 pieces of aphyric basalt with a 5x5x5 cm xenolith. Despite many bites, 22 DS contained merely 3 rocks of basalt and dolerite, showing alteration zoning, plagioclase and clinopyroxene, altered olivine, rare vesicles and Mn-crust. The next dredge contained altered lava flows, pillows and basalt with abundant olivine phenocrysts as well as thick glass crusts and small alteration haloes. 29 DS at 1.4 Ma contained mainly aphyric basalt with very rare plagioclase phenocrysts, alteration zoning and thick glass + Mn-crust. One piece contained alteration haloes. The next dredge showed more altered rocks with nearly the same composition. Aphyric basalts with weathered glass or Mn-crust at 36 DS

are much more altered with rare phenocrysts (one piece with plagioclase spherulites) and vesicles filled with clay or Fe-oxyhydroxide. Despite many bites 41 DS returned empty. At 7.0 and 8.8 Ma, rocks consisiting of basalt and dolerite with plagioclase and altered olivine, Fe-staining, vesicles, alteration zoning, alteration haloes and brownish altered glass crust, some with Mn-crust as well were recovered. A breccia with basalt fragments was found at 7.0 Ma. Rocks at 8.8 Ma show thicker Mn-crusts.
In addition to dredging, some small rock and glass pieces were collected by coring (Table 4.2).

Station number	Latitude °S	Longitude °W	Water Depth	Age (Ma)	cm above base
7 DL	14°55,21 S	109°10,32 W	3486	4.6	300
12 DL	14°33,67 S	111°15,20 W	3194	1.7	base
27 DL	14°16,54 S	112°19,44 W	3043	0.5	core catcher
37 DL	14°56,61 S	109°11,51 W	3699	4.6	230
38 DL	14°54,94 S	109°10,73 W	3541	4,6	130 – 20 - base
40 DL	14°55,52 S	109°10,65 W	3582	4,6	core catcher
40 DL	14°55,52 S	109°10,65 W	3582	4,6	turbidite at 260

Table 4.2: Rocks found by coring.

5. Water sampling by CTD

5.1 Input of arsenic to the water column by hydrothermal fluids

Christian Scholz, (Prof. M. Isenbeck-Schroeter, Uni. Heidelberg)

Arsenic is extensively cycled at the earth´s surface and has a complex marine geochemistry. It has multiple oxidation states and is present in the oceanic environment as both inorganic and organic complexes, which are interconverted through chemical and biological activity. The aim of our study is to identify and quantify the flux of As into the marine environment with particular reference to input from hydrothermal sources.
A recently submitted proposal to the EU is seeking to investigate the input of As from shallow hydrothermal systems. SONNE cruise 145-2 to the East Pacific Rise 14°S gave us the opportunity to collect water-column samples in close proximity to the ridge axis, to obtain information about input of As from hydrothermal systems in the deep-sea. Questions to be addressed are firstly whether it is possible to detect a hydrothermal signal in the open ocean. Secondly, we will attempt to distinguish analytically between different oxidation states in order to obtain information about the redox-behaviour of As in the marine environment.
Analysis of water samples from SONNE cruise 145-2 will be conducted at the Institute for Environmental Geochemistry in Heidelberg, Germany.

5.2 Sampling description

On this cruise we took samples of the water column by CTD at two stations (4 CTD and 19 CTD). The first sampling point (Station 4CTD, Figure 5.1) at 106° 8,48 W and 15° 45,78 S and a water depth of 3836 m is in the area of 8 million years old oceanic crust. Heat flow in this area is low, so the hydrothermal input should be small to non-existent. This gives us the possibility to get a first hint about the normal background of the compounds of interest in the sampling section. We took 24 samples in a profile across the whole water column (for details see Table 5.1). The water- column near the ocean floor is of major interest for us, as the dilution of any hydrothermal signal in the overlying seawater should increase with distance to the seafloor. The sampling profile began close to the seafloor with sampling steps of a few meters, increasing to sampling steps of 250 m in the upper regions. When the CTD was back on board we measured pH and Eh of every sample, this data are also listed in Table 5.1.
The second sampling point (Station 19CTD) at 112° 30,84 W and 14° 9,18 S and a water depth of 2622 m is in the area of the spreading centre. At this sampling point we hope to get higher upflow of hydrothermal fluids. If this is the case, we hope to get information about the hydrothermal input of the compounds of interest. The specific data of sampling and measurement are shown in Table 5.2 and Figure 5.2. The measurement of pH and Eh on board was not possible, as there was a defect on the voltmeter.
All samples have been stored at 4° C in a cooling room to await refrigerated transport to the home laboratory.

Table 5.1: Specific data of sampling; station 4CTD

sample	water depth (m)	T (°C)	conductivity (mS)	O_2 (mg/l)	pH	Eh (mV)
I-24	3830	1,84	31,95	5,2	7,8	430
I-23	3827	1,84	31,95	5,2	7,8	427
I-22	3824	1,84	31,95	5,2	7,8	418
I-21	3820	1,84	91,94	5,2	7,8	422
I-20	3815	1,84	31,94	5,2	7,8	428
I-19	3810	1,84	31,94	5,2	7,8	431
I-18	3780	1,84	31,93	5,2	7,7	431
I-17	3755	1,84	31,92	5,2	7,8	439
I-16	3730	1,83	31,91	5,2	7,8	438
I-15	3630	1,83	31,86	5,2	7,8	441
I-14	3330	1,80	31,73	5,2	7,8	441
I-13	3080	1,80	31,64	5,3	7,8	441
I-12	2830	1,80	31,54	5,3	7,8	441
I-11	2580	1,82	31,46	5,4	7,8	443
I-10	2330	1,89	31,42	5,3	7,8	446
I-9	2080	2,07	31,46	4,9	7,7	446
I-8	1830	2,39	31,62	4,2	7,7	446
I-7	1580	2,79	31,86	3,6	7,7	448
I-6	1330	3,32	32,18	3,1	7,7	452
I-5	1080	4,05	32,69	2,5	7,6	453
I-4	830	5,20	33,57	1,8	7,6	452
I-3	580	6,92	35,04	1,5	7,6	450
I-2	330	10,84	38,56	0,8	7,7	453
I-1	80	22,14	51,47	7,5	8,1	427

Figure 5.1: CTD-data of the water column at station 4CTD

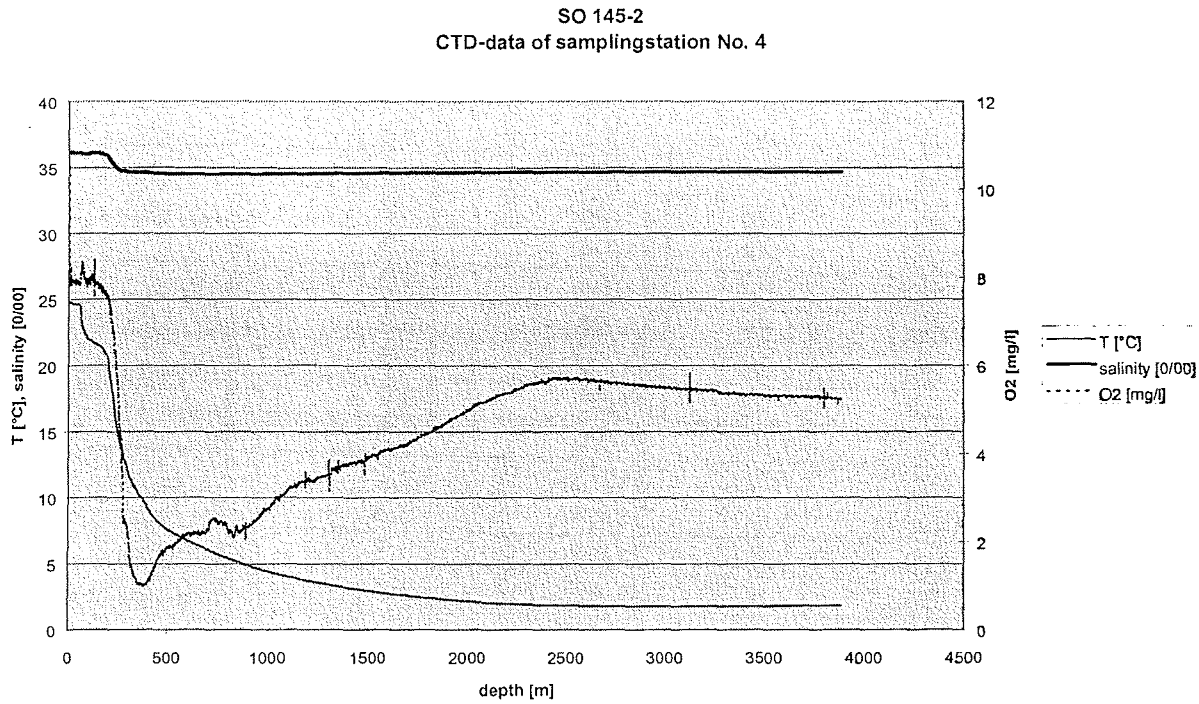

Figure 5.2: CTD-data of the water column at station 19CTD

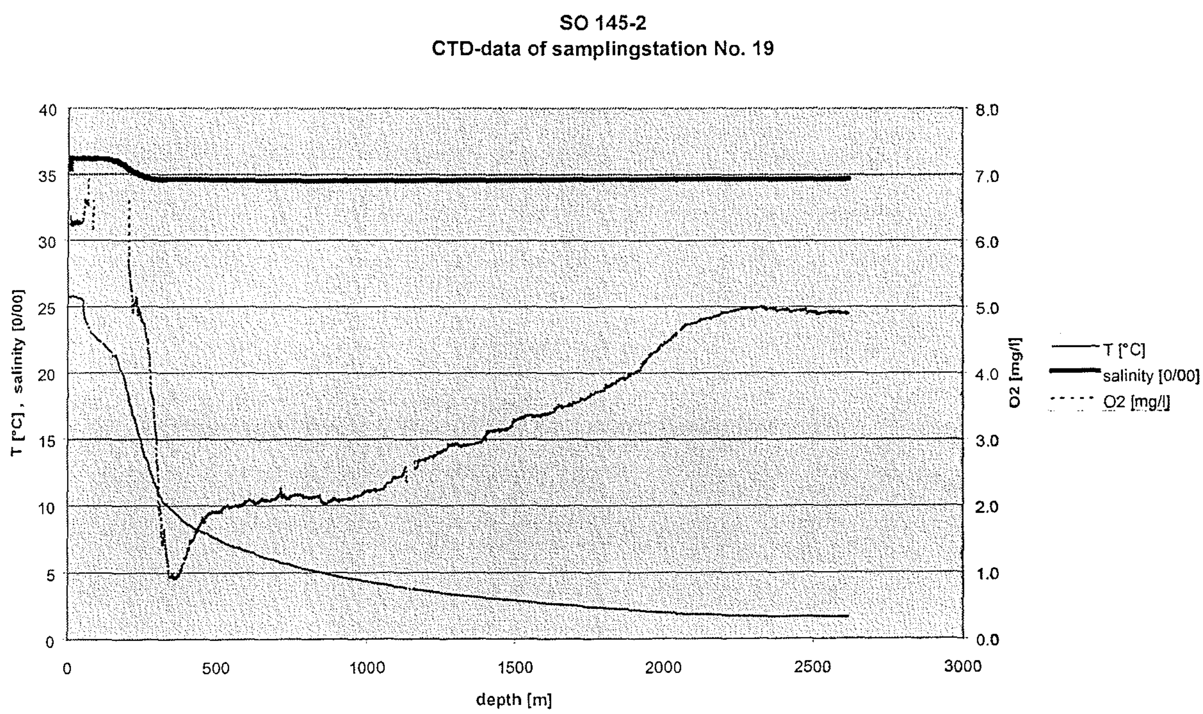

Table 5.2: Specific data of sampling; station 19CTD

sample	water depth (m)	T (°C)	conductivity (mS)	O_2 (mg/l)	pH	Eh (mV)
II-24	2622	1,84	31,49	4,9	-	-
II-23	2619	1,83	31,49	4,9	-	-
II-22	2616	1,83	31,49	4,9	-	-
II-21	2612	1,84	31,49	4,9	-	-
II-20	2607	1,84	31,49	4,9	-	-
II-19	2602	1,83	31,48	4,9	-	-
II-18	2587	1,83	31,47	4,9	-	-
II-17	2570	1,85	31,48	4,9	-	-
II-16	2545	1,85	31,47	4,9	-	-
II-15	2520	1,85	31,46	4,9	-	-
II-14	2470	1,85	31,44	4,9	-	-
II-13	2370	1,85	31,40	4,9	-	-
II-12	2270	1,89	31,39	4,9	-	-
II-11	2170	1,95	31,39	4,8	-	-
II-10	2000	2,14	31,48	4,4	-	-
II-9	1850	2,37	31,61	3,9	-	-
II-8	1600	2,81	31,88	3,3	-	-
II-7	1250	3,62	32,19	2,7	-	-
II-6	1150	3,89	32,58	2,6	-	-
II-5	900	4,88	33,33	2,0	-	-
II-4	650	6,26	34,49	2,0	-	-
II-3	350	9,55	37,46	0,8	-	-
II-2	100	22,48	52,01	6,5	-	-
II-1	20	25,66	55,44	6,2	-	-

6. Haloacetic acids in the marine environment

Jens Pracht, (M. Isenbeck- Schroeter, H.F. Schoeler, I. Fahimi, B. Scott)

6.1 Introduction

Haloacetates are a group of compounds comprising chloro- bromo-, and fluoroacetates. Such compounds are polar, highly soluble in water and strongly acidic.
Generally, it is recognised that haloacetates are widespread in the aquatic environment. They have been detected in rainwater, snow, glacier ice, ground water and surface water.
This has caused some concern, because chloroacetates and trifluoracetate are highly phytotoxic. The present concentrations e.g. of TFA in precipitation are far below the toxic level, but a few samples taken from rain water in Central Europe showed concentrations close to toxic levels.
However, little is known about their concentrations in marine environments, especially in the water column. A few vertical profiles exist so far, for the Atlantic and the Arctic Ocean, but nothing is known about the Pacific.
Therefore, 2 water profiles, each with 24 samples taken at various depths (see Chapter 5), were collected and will be analysed for haloacetic acids at the Instiut of Environmental Geochemistry in Heidelberg(*) and at the National Water Research Institute, Burlington(°), Ontario, Canada.
The main objectives of the present research is to investigate the occurence and distribution of haloacetates in the marine environment.

6.2 Sources

It is generally accepted that an important anthropogenic source of chloroacetates exists. They are used as chemicals in modern society but can also be produced as by- products during chlorination processes (e.g. detoxification of cyanide, bleaching of paper and water disinfection). A further source is atmospheric photooxidation of C_2 chlorocarbons, in particular trichlorethene, tetrachlorethene and 1,1,1-trichlorethane. These have been produced, in millions of tonnes, since the early 30s by the chemical industry, where they are mainly used as solvents and degreasing agents.
But this anthropogenic source cannot be the whole story, it appears that these sources are insufficient to explain the prevalence of haloacetates, and there are some suggestions that chloroacetates and even TFA may originate from natural sources as well.
By investigating different ice cores which represent natural archives of precipitation, it has been shown that in pre- industrial time, long before large scale industrial production of elemental chlorine and chlororganics began, natural backround concentrations of these compounds existed.

There are strong indications that a natural source of halocatetates exists, but the underlying process- be it biotic or abiotic- is still unknown.

For example, for the volatile halogenated organic compounds biological productivity in the oceans has been implicated as as one of the main natural sources. Also

volcanic emissions and abiotic oxidation processes in soils and sediments play a very important role.
We suggest that similar processes, creating volatile halocarbons, could also produce these polar haloacetic compounds.
Therefore it was for these reasons that we collected our water samples near to and just above the East Pacific Rise. If an interaction between the volcanic activity and, or the sediments/ porewater and organic material occurs, which produces halocarbons, they should be detected in our water samples. Therefore we decided to take samples at high resolution near the seafloor.

7. He isotope analysis: Determinimg the ridge flank flux of uranium and seawater.

Rachel Dunk, Zoë Bond.

7.1 Introduction

^{238}U and ^{235}U are primordial radionuclides and are the parents of two of the three naturally occuring radioactive uranium decay series. The third naturally occuring isotope ^{234}U, is a product in the decay series of ^{238}U. Of these 3 isotopes ^{238}U, with a half life of 4500 Ma, is the most abundant in nature, accounting for greater than 99% of the total U inventory. ^{235}U, with a half life of 710Ma, accounts for less than 1% and ^{234}U, with the much shorter half life of 248Ka, is present only in trace amounts from the decay of ^{238}U.

^{238}U and ^{235}U decay via emission of alpha (helium nuclei, ^{4}He) and beta (electron) particles, producing a variety of daughters whose half lives range from seconds to thousands of years. The different physico-chemical properties of the ^{238}U and ^{235}U parents and their daughters can lead to separation (fractionation) of these radionuclides, thus giving rise to radioactive disequilibrium. This U series disequilibrium forms the basis of many geochemical methods of studying processes in the marine environment.

The distribution of U in the oceans and the source and sink terms are of particular interest to the geochemist because of the extensive use of U daughter nuclides as tracers and time indices of many oceanographic processes. As a heat producing element U is also of importance to studies of mantle structure and earth evolution.

It would appear that the oceans have been in steady state with respect to U (with concentrations remaining constant) for at least the last 4Ma. Consideration of the global oceanic geochemical U budget suggests that uptake of U during low temperature hydrothermal alteration of relatively young oceanic crust may be an important sink. Removal of U probably occurs via reduction of U to the insoluble tetravalent oxide UO_2 and subsequent adsorption to rock surfaces or incorporation into authigenic minerals. Although the removal of U during on-axis hydrothermal circulation through ocean ridge systems may be considered quantitative [*Michard and Albarède*, 1985], as yet relatively little is known about the behaviour of U during low temperature off-axis hydrothermal circulation. Recently, low temperature fluids (basement exit temperature of 64°C) have been analysed for U content and U removal appears to be virtually complete.

We propose to measure the ^{4}He (alpha particle) flux, produced by the decay of crustally sequestered U, through sediments overlying the ridge flanks. This will be done by measuring the pore water gradient in $^{3}He/^{4}He$. Since the isotopic ratio of uranigenic He is extremely low compared to atmospheric and mantle derived He, this type of measurement is more sensitive and less ambiguous than reliance soley on concentration anomalies. We argue that this uranigenic He flux would provide a measure of the total amount of U within the sediments and crust below. If U removal is near-quantitative during low temperature hydrothermal circulation this would also provide a minimum constraint on the integrated volume flux of seawater through the crust.

7.2 Sample collection

Samples were collected from the following cores (see Appendix 5 for core descriptions):

8Ma Crust: 3, 29, 30
4Ma Crust: 4-7, 25, 28
1.5Ma Crust: 8-10, 23
0.3Ma Crust: 11-14

7.3 He samples

He is a sufficiently rapidly diffusing gas that significant compromise of a sediment core occurs almost immeadiately after coring. However, this compromise is more pronounced in the outer perimeter of the core. To circumvent this problem, as soon as the sediment core arrived on deck, small (10cm) sections of sediment core were cut (at ca. 50cm intervals) and subcored axially through the centre of the section using a 10mm OD copper tube. The copper tube was then crimp sealed (to expel a minimum of 1cm of sediment from both ends of the tube) to form a temporary vacuum tight seal. Some problems were experienced in forming the seals on the sub-core tubes. When the second seal was made the resultant increase in internal pressure in the tube led on occasion to forced leaks in a seal. A second problem was also experienced when sub-coring through foram rich sediments with a coarse sandy texture. In this case sediment grains/forams forced holes in a seal or prevented complete closure of a seal. The seals on all samples were therefore also coated with epoxy resin (an effective barrier to He diffusion).

These samples will be analysed in the Noble Gas Laboratory at the Southampton Oceanography Centre under the supervision of Prof. W. Jenkins.

7.4 Sediment samples

Samples were collected from the remaining sediment in the 10cm core sections to analyse for solid state U and Th. This will allow a correction to be applied to the measured $^3He/^4He$ flux for in-situ radioactive production of He in the sediments.

Literature cited

Grevemeyer, I., and W. Weigel, Increase of seismic velocities in upper oceanic crust: The "superfast" spreading East Pacific Rise at 14°14'S, *Geophys. Res. Lett.*, *24*, 217-220, 1997.

Grevemeyer, I., W. Weigel, and C. Jennrich, Structure and aging of the oceanic crust at 14°S on the East Pacific Rise, *Geophys. J. Int.*, *135*, 573-584, 1998.

Michard, A., and F. Albarède, Hydrothermal uranium uptake at ridge crests, *Nature*, *317*, 244-246, 1985.

Villinger, H.e.a., Report and preliminary results of Sonne cruise 145-1 Balboa - Talcahuano 21.12.1999-28.01.2000, *Berichte Fachbereich Geowissenschaften, Univ. Bremen*, *154*, 147pp, 2000.

Weigel, W., I. Grevemeyer, N. Kaul, H. Villinger, T. Lüdmann, and H.K. Wong, Aging of oceanic crust at the southern East Pacific Rise, *Eos*, *77*, 504, 1996.

Appendix 1: Station List

STATION LIST

Date	Time on bottom UTC	Station-Nr.	Lat.	Long.	Water depth (m)	Device	Length of core (m)	Core recovery (m)
12.02.00	14:33	1	15°46,98 S	106°10,58 W	3870	SL	9	4,8
"	18:15	2	15°47,22 S	106°10,41 W	3879	SL	6	3,9
"	21:24	3	15°45,79 S	106°08,48 W	3847	SL	6	5,0
13.02.00	00:07	4	15°45,78 S	106°08,49 W	3847	CTD	24 bottles	
"	18:09	5	14°55,86 S	109°10,91 W	3633	SL	6	4,3
"	20:55	6	14°54,94 S	109°10,75 W	3525	SL	6	1,9
"	23:30	7	14°55,21 S	109°10,32 W	3486	SL	6	4,9
14.02.00	02:28	8	14°58,29 S	109°12,90 W	3733	SL	6	5,9
"	ca. 11:00	9	14°52,41 S	110°32,22 W	3208	DS		full
"	18:45	10	14°33,89 S	111°18,74 W	3318	SL	6	4,5
"	21:21	11	14°34,54 S	111°16,02 W	3190	SL	6	5,75
"	23:42	12	14°33,67 S	111°15,20 W	3194	SL	6	5,75
15.02.00	ca. 4:30	13	14°43,82 S	111°51,27 W	3280	DS		empty
"	12:40	14	14°16,82 S	112°20.09 W	3164	SL	6	5,47
"	15:03	15	14°16,48 S	112°19,38 W	3047	SL	6	4,3
"	17:33	16	14°16,72 S	112°20,36 W	3100	SL	6	2,7
"	19:52	17	14°16,94 S	112°20,41 W	3100	SL	6	3,6
"	22:48	18	14°15,82 S	112°32,65 W	2653	DS		full
16.02.00		19	14°09,18 S	112°30,84 W	2622	CTD	24 bottles	
"	04:10	20	14°09,17 S	112°30,83 W	2650	DS		full
"	07:50	21	14°05,16 S	112°30,19 W	2645	DS		full
"	13:10	22	14°11,64 S	112°27,79 W	3086	DS		3 rocks
"	17:13	23	14°16,47 S	112°19,44 W	3041	SL	6	3,8
"	19:26	24	14°16,20 S	112°19,28 W	3057	SL	6	4,06
"	21:43	25	14°16,88 S	112°19,84 W	3089	SL	6	3,8
17.02.00	00:04	26	14°16,73 S	112°19,44 W	3061	SL	6	4,68
"	02:15	27	14°16,54 S	112°19,44 W	3043	SL	6	3,28
"	05:40	28	14°08,52 S	112°06,64 W	3128	DS		10%
"	-	29	14°49,48 S	111°54,41 W	3355	DS		full
"	20:39	30	14°34,30 S	111°17,10 W	3239	SL	6	5,7
"	22:55	31	14°34,42 S	111°16,56 W	3209	SL	6	5,75
18.02.00	01:09	32	14°34,85 S	111°16,02 W	3194	SL	6	5,75
"	03:22	33	14°34,66 S	111°15,47 W	3211	SL	6	5,75
"	05:43	34	14°33,75 S	111°14,79 W	3184	SL	6	5,75
"	10:19	35	14°35,76 S	110°45,95 W	3333	DS		15 rocks
"	23:42	36	14°53,54 S	109°11,22 W	3503	DS		25 rocks
19.02.00	06:01	37	14°56,61 S	109°11,51 W	3699	SL	6	5,95
"	08:44	38	14°54,94 S	109°10,73 W	3541	SL	6	1,5
"	12:11	39	14°56,24 S	109°11,17 W	3675	SL	6	5,9
"	14:50	40	14°55,52 S	109°10,65 W	3582	SL	6	5,75
"	19:48	41	15°06,38 S	108°42,61 W	3715	DS		empty
20.02.00	06:41	42	15°23,05 S	107°22,01 W	3873	DS		10%
"	15:56	43	15°17,52 S	106°18,13 W	4113	DS		full
"	23:45	44	15°47,12 S	106°10,00 W	3886	SL	6	5,65
21.02.00	02:55	45	15°47,12 S	106°09,59 W	3884	SL	12	5,1

Appendix 2: Description of dredge samples

Station: SO145-2 9 DS **Date:** 14-2-00
Location (which area): Ocean crust at 3 Ma

		Latitude °S	Longitude °W	Cable length	Water Depth
On bottom		14°52.38	110°32.91	3379 m	3419 m
Off bottom		14°52.43	110°32.21	3268 m	3212 m

Sample description

Sample	Size (cm)	Description (glass?, vesicles?, altered? what samples taken?)
9DS-1		Dolerite, ~ 1 mm alteration crust, vesicles, yellowish brown alteration Samples: TS, GC
9DS-2		Aphyric glassy pillow fragment with yellowish brown alteration Samples: Glass
9DS-3	10 x 10 x 10	Aphyric dolerite with alteration zoning Samples : TS, GC
9DS-4		Aphyric dolerite with a glass crust and alteration zoning Samples : Glass, TS, GC
9DS-5		Dolerite, vesicles filled with clay, alteration zoning, Mn crust Samples : TS, GC
9DS-6		Basalt with an altered glass crust Samples : TS, GC
9DS-7		Strongly altered glass Samples : TS, GC
9DS-8		Dolerite, vesicles, yellowish brown alteration, Mn crust Samples : TS, GC, Glass
9DS-9		Dolerite, vesicles, strong alteration, Mn crust, in some places glass occur
9DS-10		Dolerite, two distinct alteration seams Samples : TS, GC
9DS-11		Dolerite, glass crust, alteration zoning Samples : Glass
9DS-12		Altered basalt core, rare plagioclase phenocrysts, alteration zoning Samples : TS, GC
9DS-13		Altered basalt core, rare plagioclase phenocrysts, alteration zoning Samples : TS, GC

Station: SO 145-2 13DS **Date:** 15-2-00
Location (which area): Ocean crust at 1.3 Ma

		Latitude °S	Longitude °W	Cable length	Water Depth
On bottom		14°43.81	111°51.27	3275 m	3280 m
Off bottom		14°43.87	111°51.14	3096 m	3118 m

Sample description : EMPTY

Station : SO 145-2 18DS **Date** : 15-2-00
Location (which area) : Ridge axis at 0.2 Ma

		Latitude °S	Longitude °W	Cable length	Water Depth
On bottom		14°15.82	112°32.65	2632 m	2653 m
Off bottom		14°14.89	112°32.61′	3080 m	2653 m

Sample description

Sample	**Size (cm)**	**Description (glass ?, vesicles ?, altered ? what samples taken ?)**
18DS-1	20 x 15 x 10	Pillow fragment with rare olivine phenocrysts, 1 mm Fe- and Mn-oxide on the surface Samples : TS, Glass
18DS-2	20 x 15 x 8	Basalt with rare plagioclase phenocrysts, 2mm glass crust, some Fe-oxide staining Samples : TS, Glass
18DS-3	10 x 10 x 5	Aphyric basalt, 1 mm glass crust, porous transition Samples : TS, Glass
18DS-4	8 x 4 x 4	Basalt with rare plagioclase phenocrysts, no glass, 1 mm Mn crust Samples : TS
18DS-5	20 x 5 x 5	Basalt with rare plagioclase and olivine phenocrysts, 1 mm glass crust, iron oxide staining, Samples : TS, Glass
18DS-6	15 x 15 x 15	Pillow fragment with 2–3 mm glass crust Samples : TS, Glass
18DS-7	10 x 10 x 5	Basalt with rare plagioclase and olivine ? phenocrysts, vesicles, 1 mm glass crust Samples : TS, Glass
18DS-8	10 x 10 x 10	2 pieces of aphyric basalt with a 5 x 5 x 5 cm xenolith (olivine+plagioclase+ vesicular magma)
18DS-9	10 x 10 x 5	Basalt with rare plagioclase, 3 mm glass crust, some white hydrothermal staining Samples : TS, Glass

Station : SO 145-2 20DS **Date** : 16-2-00
Location (which area) : Ridge axis at 0.2 Ma

		Latitude °S	Longitude °W	Cable length	Water Depth
On bottom		14°09.23	112°30.90	2607 m	2648 m
Off bottom		14°10.06	112°31.20	2630 m	2644 m

Sample description

Sample	**Size (cm)**	**Description (glass ?, vesicles ?, altered ? what samples taken ?)**
20DS-1	20 x 15 x 15	Basalt with olivine phenocrysts, rare plagioclase phenocrysts, 1 mm glass crust Samples : TS, Glass
20DS-2	10 x 10 x 5	Basalt with rare olivine and plagioclase phenocrysts, small vesicles Samples : TS
20DS-3	10 x 10 x 5	Basalt, 1 mm glass crust, vesicles, very rare olivine phenocrysts Samples : TS, Glass
20DS-4	30 x 25 x 10	Basalt with rare plagioclase and olivine phenocrysts, 2-3 mm glass crust, vesicles near rim, Fe-staining Samples : TS, Glass
20DS-5	20 x 5 x 5	Basalt with very rare plagioclase and olivine phenocrysts, 1 mm glass crust, vesicles near rim, yellowish brown iron oxide Samples : TS, Glass

Station : SO 145-2 21DS **Date** : 16-2-00
Location (wich area) : Ridge axis at 0.2 Ma

		Latitude °S	Longitude °W	Cable length	Water Depth
On bottom		14°05.18	112°30.18	2665 m	2643 m
Off bottom		14°06.05	112°30.18	2562 m	2677 m

Sample description

Sample	**Size (cm)**	**Description (glass ?, vesicles ?, altered ? what samples taken ?)**
21DS-1	25 x 8 x 20 cm	Sheet flow with rare 1-2 mm plagioclase phenocrysts, some vesicles, 2-3 mm glass crust Samples : TS, Glass
21DS-2	30 x 20 x 10 cm	Pillow fragment, small vesicles near rim, 1-4 mm glass crust, rare plagioclase phenocrysts Samples : TS
21DS-3	5 x 5 x 5 cm	Basalt with 1-2 mm glass crust, rare olivine phenocrysts, some iron oxide staining Samples : TS, Glass
21DS-4	30 x 25 x 10 cm	Vesicular basalt, very thin glass crust, some manganese oxide on the surface Samples : TS, Glass
21DS-5	5 x 5 x 5 cm	Pillow segment with vesicles, 2 mm glass crust, rare plagioclase phenocrysts Samples : TS, Glass

Station : SO 145-2 22DS **Date** : 16-2-00

Location (which area) : Ocean crust at 0.4 Ma

		Latitude °S	Longitude °W	Cable length	Water Depth
On bottom		14°11.64	112°27.79	3086 m	3088 m
Off bottom		14°11.65	112°27.46	2853 m	2923 m

Sample description :

Sample	Size (cm)	Description (glass ?, vesicles ?, altered ? what samples taken ?)
22DS-1	20 x 15 x 10	Basalt, rare plagioclase phenocrysts, rare vesicles, alteration zoning, manganese crust Samples : TS, GC
22DS-2	15 x 15 x 5	Dolerite, alteration haloes, clinopyroxene and plagioclase phenocrysts, altered olivine Samples : TS, GC
22DS-3	10 x 10 x 10	Basalt, rare plagioclase phenocrysts, rare vesicles, alteration zoning, manganese crust, altered olivine Samples : TS, GC

Station : SO 145-2 28DS **Date:** 17-2-00
Location (which area) **:** Ocean crust at 0.75 Ma

		Latitude °S	Longitude °W	Cable length	Water Depth
On bottom		14°08.52	112°06.64	3127 m	3128 m
Off bottom		14°08.34	112°06.08	2930 m	2945 m

Sample description :

Sample	**Size (cm)**	**Description (glass ?, vesicles ?, altered ? what samples taken ?)**
28DS-1	25 x 20 x 20	Basalt, abundant olivine phenocrysts, vesicles, 4-5 mm glass crust, rare plagioclase phenocrysts, Fe staining Samples : TS, GC, Glass
28DS-2	30 x 15 x 5	Glassy, altered lava flow, 1 mm Mn crust, rare vesicles Samples : TS, GC, Glass
28DS-3	12 x 10 x 10	Basalt, abundant olivine phenocrysts, vesicles, glass crust, rare clinopyroxene and plagioclase phenocrysts, Fe staining Samples : TS, GC, Glass
28DS-4	10 x 10 x 5	Basalt, abundant olivine phenocrysts, abundant alteration haloes (1-2 mm), 5 mm glass crust, Fe staining, vesicles Samples : TS, GC, Glass
28DS-5	10 x 10 x 10	Pillow, 1 mm Mn crust, abundant alteration haloes (1 mm), rare vesicles, rare olivine phenocrysts Samples : TS, GC, Glass
28DS-6	10 x 8 x 8	Basalt, olivine phenocrysts, vesicles, 1 mm Mn crust, rare clinopyroxene and plagioclase phenocrysts Samples : TS, Glass

Station : SO 145-2 29DS **Date :** 17-02-00
Location (which area) : Ocean crust at 1.4 Ma

		Latitude °S	Longitude °W	Cable length	Water Depth
On bottom		14°49.43	111°54.41	3345 m	3355 m
Off bottom		14°49.48	111°53.81	3110 m	3122 m

Sample description :

Sample	Size (cm)	Description (glass ?, vesicles ?, altered ? what samples taken ?)
29DS-1	30 x 20 x 20	Basalt, rare vesicles, rare plagioclase phenocrysts, alteration zoning, Mn crust Samples : TS, GC, Glass
29DS-2	20 x 20 x 20	Aphyric basalt, 2 mm glass crust, 1 mm Mn crust, very rare vesicles, alteration zoning Samples : TS, GC, Glass
29DS-3	15 x 10 x 10	Aphyric basalt, 1 mm glass crust, alteration zoning, Fe staining Samples : TS, GC, Glass
29DS-4	10 x 10 x 5	Aphyric basalt, very rare plagioclase phenocrysts, 1-10 mm glass crust, rare vesicles, 1-10 mm Mn crust Samples : TS, GC, Glass
29DS-5	20 x 20 x 15	Basalt, plagioclase phenocrysts, very thin glass crust (1 mm), Mn crust, alteration zoning Samples : TS, GC
29DS-6	30 x 30 x 20	Aphyric basalt, very rare plagioclase phenocrysts, 5-15 mm Mn crust, alteration zoning Samples : TS, GC
29DS-7	8 x 5 x 3	Aphyric basalt, rare plagioclase phenocrysts, vesicles near rim, 1 mm Mn crust, alteration zoning, Fe staining Samples : TS, GC
29DS-8	5 x 5 x 5	Aphyric basalt, rare vesicles, alteration haloes (1 mm) Samples : TS, GC
29DS-9	10 x 5 x 5	Aphyric basalt, very rare plagioclase phenocrysts, vesicles, alteration zoning, Fe staining Samples : TS, GC
29DS-10	25 x 25 x 20	Aphyric basalt, very rare plagioclase phenocrysts, vesicles, 1-4 mm glass crust, thin Mn crust Samples : TS, GC, Glass

Station : SO 145-2 35DS **Date :** 18-2-00
Location (which area) : Seamount at 2.8 Ma

		Latitude °S	Longitude °W	Cable length	Water Depth
On bottom		14°35.75	110°45.95	3350 m	3333 m
Off bottom		14°36.09	110°45.45	3020 m	3050 m

Sample description :

Sample	**Size (cm)**	**Description (glass ?, vesicles ?, altered ? what samples taken ?)**
29DS-1	10 x 10 x 10	Aphyric basalt, very rare plagioclase phenocrysts, 3 mm Mn crust, alteration haloes, rare vesicles, 1 mm brownish altered glass crust Samples : TS, GC
29DS-2	8 x 5 x 3	Aphyric basalt, rare plagioclase phenocrysts, vesicles near rim, 1-10 mm Mn crust, 2 mm glass crust, alteration haloes, large vesicles filled with clay Samples : TS, GC, Glass
29DS-3	10 x 10 x 10	Aphyric basalt, very rare plagioclase phenocrysts, Fe staining, small vesicles, alteration zoning, 4 mm Mn crust Samples : TS, GC
29DS-4	10 x 10 x 10	Aphyric basalt, very rare plagioclase phenocrysts, vesicles, alteration haloes, brownish altered glass (1 mm) Samples : TS, GC
29DS-5		Several small basalt fragments

Station: SO 145-2 36DS **Date:** 18-2-00
Location (which area) **:** Ocean crust at 4.6 Ma

		Latitude °S	Longitude °W	Cable length	Water Depth
On bottom		14°53.54 S	109°11.22	3478 m	3499 m
Off bottom				2876 m	2921 m

Sample description :

Sample	Size	Description (glass ?, vesicles ?, altered ? what samples taken ?)
36DS-1	20x15x15	Basalt, rare plagioclase phenocrysts, very rare olivine phenocrysts, small vesicles near rim, thin glass crust (< 1mm), alteration zoning Samples : TS, GC
36DS-2	10x10x10	Basalt, rare plagioclase phenocrysts, brownish alteration zoning, vesicles (up to 4 mm) filled with clay or Fe-oxyhydroxide Samples : TS, GC
36DS-3	15x10x8	Basalt, rare plagioclase phenocrysts, alteration zoning, vesicles (1 to 4 mm) filled with clay or Fe-oxyhydroxide, Mn-crust, Samples : TS, GC.
DS36-4	10x25x16	Aphyric basalt, very rare plagioclase phenocrysts, Fe-staining, brownish altered glass, thin Mn-crust Samples : TS, GC
36DS-5	6x6x6	Basalt, rare plagioclase phenocrysts, brownish alteration zoning, vesicles (up to 4 mm) filled with clay or Fe-oxyhydroxide Samples : TS, GC
36DS-6	10x10x5	Aphyric basalt, very rare olivine phenocrysts, Fe-oxyhydroxide, alteration zoning, small alteration haloes (<1 mm), vesicles (~ 2 mm), thin glass-crust (~ 1 mm), Mn-crust Samples : TS, GC
36DS-7	10x5x5	Basalt, plagioclase spherulite (1-2 mm), vesicles (~ 4 mm) filled with clay or Fe-oxyhydroxide, glass crust (1–2) mm, Mn-crust (1-10 mm) Samples : TS, GC
36DS-8	6x6x6	Basalt, very rare plagioclase phenocrysts, small alteration haloes (~ 1 mm), vesicles filled with clay or Fe-oxyhydroxide, Fe-staining, altered glass crust (1-10 mm) Samples : TS, GC, Glass
36DS-9	7x5x3	Aphyric basalt, very rare plagioclase phenocrysts, 1 mm altered glass crust Samples : TS, GC
36DS-10	5x5x5	Aphyric basalt, very rare plagioclase phenocrysts, Fe-staining, thin, altered glass crust (<1 mm), thin Mn-crust (<1 mm) Samples : TS, GC

Station : SO 145-2 41DS **Date :** 19-2-00
Location (which area) : Seamount at 5.6 Ma

		Latitude °S	Longitude °W	Cable length	Water Depth
On bottom		15°06.37	108°42.61	3664 m	3709 m
Off bottom		15°06.37	108°42.05	3800 m	3319 m

Sample description : empty

Station : SO 145-2 42DS **Date** : 20-02-00
Location (which area) : Ocean crust at 7 Ma

		Latitude °S	Longitude °W	Cable length	Water Depth
On bottom		15°23.05	107°22.01	3865 m	3873 m
Off bottom		15°23.04	107°21.45	3550 m	3631 m

Sample description :

Sample	**Size (cm)**	**Description (glass ?, vesicles ?, altered ? what samples taken ?9**
42DS-1	20x10x8	Basalt, plagioclase phenocrysts, altered olivine phenocrysts, vesicles, Fe-staining, alteration zoning Samples : TS, GC
42DS-2	25x15x10	Basalt, plagioclase phenocrysts, altered olivine phenocrysts, vesicles, Fe-staining, 0-5 mm glass crust, alteration zoning Samples : TS, GC, Glass
42DS-3	30x20x10	Dolerite, plagioclase phenocrysts, altered olivine phenocrysts, vesicles, some Fe-staining, alteration zoning, 0-10 mm Mn-crust Samples : TS, GC
42DS-4	20x15x10	Basalt, plagioclase phenocrysts, alteration haloes (~1 mm), rare vesicles, Fe-staining, alteration zoning, brownish altered glass crust Samples : TS, GC
42DS-5	20x10x10	Basalt, very rare plagioclase phenocrysts, altered olivine phenocrysts, vesicles, some Fe-staining, alteration zoning, brownish altered glass Samples : TS, GC
42DS-6	25x20x8	Aphyric basalt, rare alteration haloes, alteration zoning Samples : TS, GC
42DS-7	25x20x20	Aphyric dolerite, some Fe-staining, alteration zoning, thin (<1 mm) Mn-crust Samples : TS, GC
42DS-8	20x15x5	Breccia including basalt fragments (1–10 mm) Samples : TS, GC
42DS-9	10x5x5	Basalt, plagioclase phenocrysts, Fe-staining, altered olivine, thin (<1 mm) altered glass crust Samples : TS, GC
42DS-10	8x5x5	Aphyric basalt, plagioclase phenocrysts, some Fe-staining, brownish altered glass crust Samples : TS, GC

Station : SO 145-2 43DS **Date** : 20-02-00
Location (which area) : Ocean crust at 8.8 Ma

		Latitude °S	Longitude °W	Cable length	Water Depth
On bottom		15°17,58	106°18.13	4096 m	4118 m
Off bottom		15°17.57	106°17.94	3850 m	4050 m

Sample description :

Sample	Size (cm)	Description
43DS-1	15x10x10	Aphyric basalt, Fe-staining, alteration zoning, Mn-crust Samples : TS, GC
43DS-2	15x10x10	Aphyric basalt, some Fe-staining, alteration zoning, thin (<1 mm) glass crust Samples : TS, GC
43DS-3	15x15x15	Aphyric basalt, some alteration haloes, alteration zoning, thin (<1 mm) Mn-crust, thin altered glass crust (<1 mm) Samples : TS, GC
43DS-4	20x10x10	Pillow, rare plagioclase phenocrysts, Fe-staining, vesicles, 1-4 mm glass crust Samples : TS, GC, Glass
43DS-5	15x10x10	Aphyric basalt, alteration haloes, thin glass crust (<1 mm) Samples : TS, GC
43DS-6	20x10x10	Dolerite, some Fe-staining, alteration zoning, thin (<1 mm) Mn-crust, breccie near rim Samples : TS, GC
43DS-7	20x8x8	Dolerite, rare plagioclase phenocrysts, some Fe-staining, alteration zoning, thin (<1 mm) brownish, altered glass crust, 3 mm Mn-crust Samples : TS, GC
43DS-8	20x20x10	Dolerite, rare plagioclase phenocrysts, some Fe-staining, alteration zoning, thin (<1 mm) Mn-crust, Samples : TS, GC
43DS-9	25x25x25	Dolerite, alteration zoning, thin (<1 mm) altered glass crust Samples : TS, GC
43DS-10	10x10x5	Aphyric basalt, very rare plagioclase phenocrysts, some Fe-staining, alteration zoning, 5-7 mm Mn-crust, interior with small vesicles, larger vesicles near rim Samples : TS, GC
43DS-11	15x10x8	Aphyric basalt, very rare plagioclase phenocrysts, alteration zoning, brownish altered glass crust (1-2 mm) Samples : TS, GC, Glass
43DS-12	20x15x15	Aphyric basalt, very rare plagioclase phenocrysts, alteration zoning, thin glass crust, thin Mn-crust, Fe-alteration haloes Samples : TS, GC
43DS-13	10x8x5	Aphyric basalt with breccia, very rare olivine phenocrysts, alteration zoning, thick glass crust (~10 mm), Fe-staining, Mn-crust (~1 mm) Samples : TS, GC, Glass
43DS-14	40x40x40	Aphyric basalt

Appendix 3: Smear slide descriptions

SMEAR SLIDES prepared and interpreted by J. Gharib (U. Hawaii)
NOTE: foraminifera fragments include both whole forams as well as partial forams (the smear slide preparation is intrinsically grain destructive)
and also calcareous fragments which might have come from other organisms but are now indistinguishable from the dominant foram fragments.
NOTE: base of core cutter is 7cm deeper than base of core catcher

Core 1SL

Sample	Height above base (cm)	cm below sea-floor	Description
C1-A	15	461	98% calcareous micrite (15% organic, 85% coccolithic) matrix, 2% amorphous silica (radiolarian) fragments
C1-B	55	421	98% calcareous micrite (15% organic, 85% coccolithic) matrix, 2% amorphous silica (radiolarian) fragments
C1-C	95	381	98% calcareous micrite (15% organic, 85% coccolithic) matrix, 2% amorphous silica (radiolarian) fragments
C1-D	150	326	95% calcareous micrite (15% organic, 85% coccolithic) matrix, 5% amorphous silica (radiolarian) fragments
C1-E	200	276	98% calcareous micrite (15% organic, 85% coccolithic) matrix, 2% amorphous silica (radiolarian) fragments
C1-F	250	226	85% micrite (40% organic-rich, 60% calcareous) matrix, 10% foraminifera fragments, 5% amorphous silica (radiolarian) fragments
C1-G	300	176	80% micrite (40% organic-rich, 60% calcareous) matrix, 10% foraminifera fragments, 10% amorphous silica (radiolarian) fragments
C1-H	340	136	80% micrite (40% organic-rich, 60% calcareous) matrix, 10% foraminifera fragments, 10% amorphous silica (radiolarian) fragments
C1-I	365	111	78% organic-rich calcareous micrite matrix, 20% foraminifera fragments, 2% amorphous silica (radiolarian) fragments
C1-L	415	61	70% organic-rich calcareous micrite matrix, 30% foraminifera fragments, <1% amorphous silica (radiolarian) fragments
C1-M	435	41	70% organic-rich calcareous micrite matrix, 30% foraminifera fragments, <1% amorphous silica (radiolarian) fragments
C1-N	450	26	70% organic-rich calcareous micrite matrix, 30% foraminifera fragments, <1% amorphous silica (radiolarian) fragments
C1-O	460	16	70% organic-rich calcareous micrite matrix, 25% foraminifera fragments, 5% amorphous silica (radiolarian) fragments
C1-P	470	6	65% organic-rich calcareous micrite matrix, 30% foraminifera fragments, 5% amorphous silica (radiolarian) fragments
	476		

Core 2SL

C2-A	15	335	93% calcareous micrite (15% organic, 85% coccolithic) matrix, 2% foraminifera fragments, 5% amorphous silica (radiolarian) fragments
C2-B	40	310	90% calcareous micrite (15% organic, 85% coccolithic) matrix, 8% foraminifera fragments, 2% amorphous silica (radiolarian) fragments
C2-C	110	240	93% calcareous micrite (15% organic, 85% coccolithic) matrrix 5% foraminifera fragments, 2% amorphous silica (radiolarian) fragments
C2-D	140	210	93% calcareous micrite (15% organic, 85% coccolithic) matrix, 5% foraminifera fragments, 2% amorphous silica (radiolarian) fragments
C2-E	185	165	90% micrite (25% organic-rich, 75% calcareous) matrix, 5% foraminifera fragments, 5% amorphous silica (radiolarian) fragments
C2-F	240	110	65% organic-rich calcareous micrite matrix, 30% foraminifera fragments, 5% amorphous silica (radiolarian) fragments
C2-G	280	70	60% organic-rich calcareous micrite matrix, 40% foraminifera fragments
C2-H	310	40	60% organic-rich calcareous micrite matrix, 40% foraminifera fragments
C2-I	335	15	65% micrite (20% organic-rich, 80% calcareous) matrix, 30% foraminifera fragments, 5% amorphous silica (radiolarian) fragments
C2-J	345	5	65% micrite (20% organic-rich, 80% calcareous) matrix, 30% foraminifera fragments, 5% amorphous silica (radiolarian) fragments
	385		(35cm double penetration)

Core 3SL

NOTE: Core #3 possibly lost up to 0.5 m from top

C3-A	10	500	96% calcareous micrite (15% organic, 85% coccolithic) matrix, 2% foraminifera fragments, 2% amorphous silica (radiolarian) fragments
C3-B	70	440	96% calcareous micrite (15% organic, 85% coccolithic) matrix, 2% foraminifera fragments, 2% amorphous silica (radiolarian) fragments
C3-C	110	400	75% micrite (50% organic-rich, 50% calcareous) matrix, 15% foraminifera fragments, 10% amorphous silica (radiolarian) fragments
C3-D	160	350	65% organic-rich calcareous micrite matrix, 30% foraminifera fragments, 5% amorphous silica (radiolarian) fragments
C3-E	200	310	70% organic-rich calcareous micrite matrix, 15% foraminifera fragments, 15% amorphous silica (radiolarian) fragments

C3-F	300	210	70% organic-rich calcareous micrite matrix, 15% foraminifera fragments, 15% amorphous silica (radiolarian) fragments
C3-G	400	110	70% organic-rich calcareous micrite matrix, 20% foraminifera fragments, 10% amorphous silica (radiolarian) fragments
C3-H	455	55	65% organic-rich calcareous micrite matrix, 30% foraminifera fragments, 5% amorphous silica (radiolarian) fragments
C3-I	485	25	70% organic-rich calcareous micrite matrix, 20% foraminifera fragments, 10% amorphous silica (radiolarian) fragments
C3-J	505	5	75% organic-rich calcareous micrite matrix, 20% foraminifera fragments, 5% amorphous silica (radiolarian) fragments
	510		

Core 5SL

C4-A	4	426	85% calcareous micrite (15% organic, 85% coccolithic) matrix,15% amorphous silica (radiolarian) fragments
C4-B	40	390	80% calcareous micrite (15% organic, 85% coccolithic) matrix, 5% foraminifera fragments, 15% amorphous silica (radiolarian) fragments
C4-C	160	270	80% calcareous micrite (15% organic, 85% coccolithic) matrix, 5% foraminifera fragments, 15% amorphous silica (radiolarian) fragments
C4-D	185	245	75% calcareous micrite (15% organic, 85% coccolithic) matrix, 10% foraminifera fragments, 15% amorphous silica (radiolarian) fragments
C4-E	300	130	70% calcareous micrite (15% organic, 85% coccolithic) matrix, 15% foraminifera fragments, 15% amorphous silica (radiolarian) fragments
C4-F	340	90	65% calcareous micrite (15% organic, 85% coccolithic) matrix, 20% foraminifera fragments, 15% amorphous silica (radiolarian) fragments
C4-G	400	30	65% calcareous micrite (15% organic, 85% coccolithic) matrix, 20% foraminifera fragments, 15% amorphous silica (radiolarian) fragments
C4-H	430	0	60% calcareous micrite (15% organic, 85% coccolithic) matrix, 25% foraminifera fragments, 15% amorphous silica (radiolarian) fragments
	430		

Core 6SL

C5-A	5	185	65% calcareous micrite (10% organic, 90% coccolithic) matrix, 25% foraminifera fragments, 10% amorphous silica (radiolarian) fragments
C5-B	75	115	65% calcareous micrite (10% organic, 90% coccolithic) matrix, 25% foraminifera fragments, 10% amorphous silica

			(radiolarian) fragments
C5-C	125	65	60% calcareous micrite (15% organic, 85% coccolithic) matrix, 30% foraminifera fragments, 10% amorphous silica (radiolarian) fragments
C5-D	155	35	55% calcareous micrite (15% organic, 85% coccolithic) matrix, 35% foraminifera fragments, 10% amorphous silica (radiolarian) fragments
C5-E	185	5	55% calcareous micrite (15% organic, 85% coccolithic) matrix, 35% foraminifera fragments, 10% amorphous silica (radiolarian) fragments
	190		

Core 7SL

C6-A	22	468	83% calcareous micrite (20% organic, 80% coccolithic) matrix, 10% foraminifera fragments, 7% amorphous silica (radiolarian) fragments
C6-B	130	360	85% calcareous micrite (15% organic, 85% coccolithic) matrix, 10% foraminifera fragments, 5% amorphous silica (radiolarian) fragments
C6-C	210	280	85% calcareous micrite (15% organic, 85% coccolithic) matrix, 10% foraminifera fragments, 5% amorphous silica (radiolarian) fragments
C6-D	280	210	75% calcareous micrite (15% organic, 85% coccolithic) matrix, 15% foraminifera fragments, 5% amorphous silica (radiolarian) fragments, 5% glass shards
C6-E	385	105	55% calcareous micrite (10% organic, 90% coccolithic) matrix, 40% foraminifera fragments, 5% amorphous silica (radiolarian) fragments
C6-F	490	0	60% calcareous micrite (10% organic, 90% coccolithic) matrix, 35% foraminifera fragments, 5% amorphous silica (radiolarian) fragments
	490		

Core 8SL

C7-A	12	568	80% calcareous micrite (20% organic, 80% coccolithic) matrix, 15% foraminifera fragments, 5% amorphous silica (radiolarian) fragments
C7-B	100	480	70% calcareous micrite (25% organic, 75% coccolithic) matrix, 20% foraminifera fragments, 10% amorphous silica (radiolarian) fragments
C7-C	165	415	75% micrite (40% organic-rich, 60% calcareous) matrix, 20% foraminifera fragments, 5% amorphous silica (radiolarian) fragments
C7-D	305	275	75% calcareous micrite (25% organic, 75% coccolithic) matrix,

			20% foraminifera fragments, 5% amorphous silica (radiolarian) fragments
C7-E	318	262	23% calcareous micrite (15% organic, 85% coccolithic) matrix, 75% foraminifera fragments, 2% amorphous silica (radiolarian) fragments
C7-F	360	220	70% calcareous micrite (20% organic, 80% coccolithic) matrix, 20% foraminifera fragments, 10% amorphous silica (radiolarian) fragments
C7-G	460	120	75% calcareous micrite (20% organic, 80% coccolithic) matrix, 15% foraminifera fragments, 10% amorphous silica (radiolarian) fragments
C7-H	475	105	2% calcareous micrite matrix, 98% foraminifera fragments
C7-I	482	98	10% calcareous micrite matrix, 90% foraminifera fragments
C7-J	490	90	83% calcareous micrite (15% organic, 85% coccolithic) matrix, 2% foraminifera fragments, 15% amorphous silica (radiolarian) fragments
C7-K	497	83	80% organic-rich calcareous micrite matrix, 15% foraminifera fragments, 5% amorphous silica (radiolarian) fragments
C7-L	579	1	75% calcareous micrite (20% organic, 80% coccolithic) matrix, 20% foraminifera fragments, 5% amorphous silica (radiolarian) fragments
	580		

Core 10SL

C8-A	12	453	70% calcareous micrite (20% organic, 80% coccolithic) matrix, 15% foraminifera fragments, 15% amorphous silica (radiolarian) fragments
C8-B	110	355	65% calcareous micrite (20% organic, 80% coccolithic) matrix, 20% foraminifera fragments, 15% amorphous silica (radiolarian) fragments
C8-C	200	265	55% micrite (40% organic-rich, 60% calcareous) matrix, 15% foraminifera fragments, 30% amorphous silica (radiolarian) fragments
C8-D	360	105	45% calcareous micrite (30% organic-rich, 70% calcareous) matrix, 25% foraminifera fragments, 20% amorphous silica (radiolarian) fragments
C8-E	460	5	55% calcareous micrite (20% organic, 80% coccolithic) matrix, 25% foraminifera fragments, 20% amorphous silica (radiolarian) fragments
	465		

Core 11SL

C9-A	15	560	55% calcareous micrite (30% organic, 70% coccolithic) matrix, 25% foraminifera fragments, 20% amorphous silica (radiolarian) fragments
C9-B	120	455	45% calcareous micrite (20% organic, 80% coccolithic) matrix, 35% foraminifera fragments, 20% amorphous silica (radiolarian) fragments
C9-C	240	335	45% calcareous micrite (20% organic, 80% coccolithic) matrix, 35% foraminifera fragments, 20% amorphous silica (radiolarian) fragments
C9-D	360	215	55% calcareous micrite (20% organic, 80% coccolithic) matrix, 25% foraminifera fragments, 20% amorphous silica (radiolarian) fragments
C9-E	480	95	55% calcareous micrite (15% organic, 85% coccolithic) matrix, 25% foraminifera fragments, 20% amorphous silica (radiolarian) fragments
C9-F	570	5	50% calcareous micrite (15% organic, 85% coccolithic) matrix, 30% foraminifera fragments, 20% amorphous silica (radiolarian) fragments
	575		

Core 12SL

C10-A	15	555	60% micrite (40% organic-rich, 60% calcareous) matrix, 25% foraminifera fragments, 15% amorphous silica (radiolarian) fragments
C10-B	120	450	55% micrite (40% organic-rich, 60% calcareous) matrix, 30% foraminifera fragments, 15% amorphous silica (radiolarian) fragments
C10-C	240	330	55% calcareous micrite (15% organic, 85% coccolithic) matrix 30% foraminifera fragments, 15% amorphous silica (radiolarian) fragments
C10-D	440	130	55% calcareous micrite (20% organic, 80% coccolithic) matrix 30% foraminifera fragments, 15% amorphous silica (radiolarian) fragments
C10-E	480	90	65% calcareous micrite (15% organic, 85% coccolithic) matrix 25% foraminifera fragments, 10% amorphous silica (radiolarian) fragments
C10-F	570	0	60% calcareous micrite (20% organic, 80% coccolithic) matrix 30% foraminifera fragments, 10% amorphous silica (radiolarian) fragments
	570		

Core 14SL

C11-A	20	520	55% organic-rich calcareous micrite matrix, 30% foraminifera fragments, 15% amorphous silica (radiolarian) fragments
C11-B	80	460	60% organic-rich calcareous micrite matrix, 25% foraminifera fragments, 15% amorphous silica (radiolarian) fragments
C11-C	160	380	65% organic-rich calcareous micrite matrix, 20% foraminifera fragments, 15% amorphous silica (radiolarian) fragments
C11-D	280	260	65% organic-rich calcareous micrite matrix, 20% foraminifera fragments, 15% amorphous silica (radiolarian) fragments
C11-E	380	160	65% organic-rich calcareous micrite matrix, 20% foraminifera fragments, 15% amorphous silica (radiolarian) fragments
C11-F	540	0	75% calcareous micrite (15% organic, 85% coccolithic) matrix, 10% foraminifera fragments, 15% amorphous silica (radiolarian) fragments
	540		

Core 15SL

C12-A	25	400	60% calcareous micrite (20% organic, 80% coccolithic) matrix, 20% foraminifera fragments, 20% amorphous silica (radiolarian) fragments
C12-B	100	325	65% micrite (40% organic, 60% coccolithic) matrix, 20% foraminifera fragments, 15% amorphous silica (radiolarian) fragments
C12-C	200	225	65% calcareous micrite (15% organic, 85% coccolithic) matrix, 20% foraminifera fragments, 15% amorphous silica (radiolarian) fragments
C12-D	265	160	60% organic-rich calcareous micrite matrix, 20% foraminifera fragments, 20% amorphous silica (radiolarian) fragments
C12-E	300	125	60% calcareous micrite (20% organic, 80% coccolithic) matrix, 20% foraminifera fragments, 20% amorphous silica (radiolarian) fragments
C12-F	420	5	55% calcareous micrite (15% organic, 85% coccolithic) matrix, 30% foraminifera fragments, 15% amorphous silica (radiolarian) fragments
	425		

Core 16SL

C13-A	20	250	40% organic-rich calcareous micrite matrix, 35% foraminifera fragments, 25% amorphous silica (radiolarian) fragments
C13-B	100	170	50% calcareous micrite (20% organic, 80% coccolithic) matrix,

			25% foraminifera fragments, 25% amorphous silica (radiolarian) fragments
C13-C	160	110	50% calcareous micrite (15% organic, 85% coccolithic) matrix, 30% foraminifera fragments, 20% amorphous silica (radiolarian) fragments
C13-D	240	30	50% calcareous micrite (20% organic, 80% coccolithic) matrix, 30% foraminifera fragments, 20% amorphous silica (radiolarian) fragments
	270		

Core 17SL

C14-A	15	350	55% micrite (40% organic, 60% coccolithic) matrix, 30% foraminifera fragments, 15% amorphous silica (radiolarian) fragments
C14-B	120	245	45% micrite (40% organic, 60% coccolithic) matrix, 35% foraminifera fragments, 20% amorphous silica (radiolarian) fragments
C14-C	220	145	45% micrite (40% organic, 60% coccolithic) matrix, 35% foraminifera fragments, 20% amorphous silica (radiolarian) fragments
C14-D	280	85	55% calcareous micrite (30% organic-rich, 70% calcareous) matrix, 30% foraminifera fragments, 15% amorphous silica (radiolarian) fragments
C14-E	360	5	55% calcareous micrite (30% organic-rich, 70% calcareous) matrix, 30% foraminifera fragments, 15% amorphous silica (radiolarian) fragments
	365		

Core 23SL

C15-A	20	374	80% calcareous micrite (20% organic, 80% coccolithic) matrix 5% foraminifera fragments, 15% amorphous silica (radiolarian fragments
C15-B	95	299	70% calcareous micrite (25% organic, 75% coccolithic) matrix 10% foraminifera fragments, 20% amorphous silica (radiolarian) fragments
C15-C	160	234	65% calcareous micrite (15% organic, 85% coccolithic) matrix 15% foraminifera fragments, 20% amorphous silica (radiolarian) fragments
C15-D	280	114	65% calcareous micrite (15% organic, 85% coccolithic) matrix 15% foraminifera fragments, 20% amorphous silica (radiolarian) fragments
C15-E	390	4	65% calcareous micrite (15% organic, 85% coccolithic) matrix 15% foraminifera fragments, 20% amorphous silica (radiolarian) fragments

	394		

Core 24SL

C16-A	15	391	70% calcareous micrite (15% organic, 85% coccolithic) matrix, 15% foraminifera fragments, 15% amorphous silica (radiolarian) fragments
C16-B	170	236	70% calcareous micrite (15% organic, 85% coccolithic) matrix, 15% foraminifera fragments, 15% amorphous silica (radiolarian) fragments
C16-C	310	96	65% calcareous micrite (15% organic, 85% coccolithic) matrix, 20% foraminifera fragments, 15% amorphous silica (radiolarian) fragments
C16-D	400	6	60% calcareous micrite (15% organic, 85% coccolithic) matrix, 25% foraminifera fragments, 15% amorphous silica (radiolarian) fragments
	406		

Core 25SL

C17-A	12	370	72% calcareous micrite (30% organic-rich, 70% calcareous) matrix, 20% foraminifera fragments, 8% amorphous silica (radiolarian) fragments
C17-B	45	337	67% calcareous micrite (20% organic, 80% coccolithic) matrix, 10% foraminifera fragments, 15% amorphous silica (radiolarian) fragments, 8% volcanic glass
C17-C	105	277	65% organic-rich calcareous micrite matrix, 15% foraminifera fragments, 20% amorphous silica (radiolarian) fragments
C17-D	230	152	65% organic-rich calcareous micrite matrix, 15% foraminifera fragments, 20% amorphous silica (radiolarian) fragments
C17-E	360	22	65% micrite (40% organic, 60% coccolithic) matrix, 20% foraminifera fragments, 15% amorphous silica (radiolarian) fragments
	382		

Core 26SL

C18-A	20	448	65% calcareous micrite (15% organic, 85% coccolithic) matrix, 20% foraminifera fragments, 15% amorphous silica (radiolarian) fragments
C18-B	140	328	60% calcareous micrite (15% organic, 85% coccolithic) matrix, 25% foraminifera fragments, 15% amorphous silica (radiolarian) fragments

C18-C	285	183	60% calcareous micrite (15% organic, 85% coccolithic) matrix, 25% foraminifera fragments, 15% amorphous silica (radiolarian) fragments
C18-D	450	18	57% calcareous micrite (15% organic, 85% coccolithic) matrix, 28% foraminifera fragments, 15% amorphous silica (radiolarian) fragments
	468		

Core 27SL

C19-A	25	301	60% calcareous micrite (25% organic, 75% coccolithic) matrix, 20% foraminifera fragments, 20% amorphous silica (radiolarian) fragments
C19-B	90	236	60% calcareous micrite (15% organic, 85% coccolithic) matrix, 20% foraminifera fragments, 20% amorphous silica (radiolarian) fragments
C19-C	180	146	60% organic-rich calcareous micrite matrix, 20% foraminifera fragments, 20% amorphous silica (radiolarian) fragments
C19-D	275	51	72% calcareous micrite (20% organic, 80% coccolithic) matrix, 20% foraminifera fragments, 18% amorphous silica (radiolarian) fragments
C19-E	320	6	67% calcareous micrite (20% organic, 80% coccolithic) matrix, 25% foraminifera fragments, 18% amorphous silica (radiolarian) fragments
	326		

Core 30SL

C20-A	20	555	70% calcareous micrite (15% organic, 85% coccolithic) matrix, 25% foraminifera fragments, 5% amorphous silica (radiolarian fragments
C20-B	130	445	70% calcareous micrite (15% organic, 85% coccolithic) matrix, 25% foraminifera fragments, 5% amorphous silica (radiolarian fragments
C20-C	255	320	75% calcareous micrite (15% organic, 85% coccolithic) matrix 20% foraminifera fragments, 5% amorphous silica (radiolarian fragments
C20-D	390	185	85% calcareous micrite (15% organic, 85% coccolithic) matrix 10% foraminifera fragments, 5% amorphous silica (radiolarian fragments
C20-E	495	80	75% calcareous micrite (15% organic, 85% coccolithic) matrix 20% foraminifera fragments, 5% amorphous silica (radiolarian fragments
C20-F	570	5	75% calcareous micrite (15% organic, 85% coccolithic) matrix 20% foraminifera fragments, 5% amorphous silica (radiolarian fragments

	575		

Core 31SL

C21-A	20	555	70% calcareous micrite (25% organic, 75% coccolithic) matrix, 20% foraminifera fragments, 10% amorphous silica (radiolarian) fragments
C21-B	125	450	65% calcareous micrite (25% organic, 75% coccolithic) matrix, 25% foraminifera fragments, 10% amorphous silica (radiolarian) fragments
C21-C	255	320	62% calcareous micrite (15% organic, 85% coccolithic) matrix, 30% foraminifera fragments, 8% amorphous silica (radiolarian) fragments
C21-D	285	290	72% calcareous micrite (15% organic, 85% coccolithic) matrix, 20% foraminifera fragments, 8% amorphous silica (radiolarian) fragments
C21-E	485	90	80% calcareous micrite (15% organic, 85% coccolithic) matrix, 15% foraminifera fragments, 5% amorphous silica (radiolarian) fragments
C21-F	570	5	80% calcareous micrite (15% organic, 85% coccolithic) matrix, 15% foraminifera fragments, 5% amorphous silica (radiolarian) fragments
	575		

Core 32SL

C22-A	15	561	80% calcareous micrite (15% organic, 85% coccolithic) matrix, 15% foraminifera fragments, 5% amorphous silica (radiolarian) fragments
C22-B	175	401	75% calcareous micrite (15% organic, 85% coccolithic) matrix, 15% foraminifera fragments, 10% amorphous silica (radiolarian) fragments
C22-C	295	281	75% calcareous micrite (15% organic, 85% coccolithic) matrix, 15% foraminifera fragments, 10% amorphous silica (radiolarian) fragments
C22-D	430	146	65% calcareous micrite (15% organic, 85% coccolithic) matrix, 25% foraminifera fragments, 10% amorphous silica (radiolarian) fragments
C22-E	570	6	65% calcareous micrite (15% organic, 85% coccolithic) matrix, 25% foraminifera fragments, 10% amorphous silica (radiolarian) fragments

Core 33SL

Note: Core #23 had overflow through top of barrel			
C23-A	20	570	70% calcareous micrite (20% organic, 80% coccolithic) matrix, 15% foraminifera fragments, 15% amorphous silica (radiolarian) fragments
C23-B	160	430	70% calcareous micrite (20% organic, 80% coccolithic) matrix, 15% foraminifera fragments, 15% amorphous silica (radiolarian) fragments
C23-C	330	260	80% calcareous micrite (15% organic, 85% coccolithic) matrix, 10% foraminifera fragments, 10% amorphous silica (radiolarian) fragments
C23-D	490	100	80% calcareous micrite (15% organic, 85% coccolithic) matrix, 10% foraminifera fragments, 10% amorphous silica (radiolarian) fragments
C23-E	585	5	75% calcareous micrite (15% organic, 85% coccolithic) matrix, 15% foraminifera fragments, 10% amorphous silica (radiolarian) fragments
	590		

Core 34SL

C24-A	25	553	80% calcareous micrite (15% organic, 85% coccolithic) matrix, 10% foraminifera fragments, 10% amorphous silica (radiolarian) fragments
C24-B	150	428	80% calcareous micrite (15% organic, 85% coccolithic) matrix, 10% foraminifera fragments, 10% amorphous silica (radiolarian) fragments
C24-C	315	263	80% calcareous micrite (15% organic, 85% coccolithic) matrix, 10% foraminifera fragments, 10% amorphous silica (radiolarian) fragments
C24-D	440	138	80% calcareous micrite (15% organic, 85% coccolithic) matrix, 10% foraminifera fragments, 10% amorphous silica (radiolarian) fragments
C24-E	575	3	80% calcareous micrite (15% organic, 85% coccolithic) matrix, 10% foraminifera fragments, 10% amorphous silica (radiolarian) fragments
	578		

Core 37SL

C25-A	20	575	96% calcareous micrite (15% organic, 85% coccolithic) matrix, 2% foraminifera fragments, 2% amorphous silica (radiolarian) fragments
C25-B	160	435	88% calcareous micrite (30% organic, 70% coccolithic) matrix, 10% foraminifera fragments, 2% amorphous silica (radiolarian) fragments
C25-C	245	350	88% calcareous micrite (30% organic, 70% coccolithic) matrix, 10% foraminifera fragments, 2% amorphous silica (radiolarian) fragments
C25-D	390	205	88% calcareous micrite (10% organic, 90% coccolithic) matrix, 10% foraminifera fragments, 2% amorphous silica (radiolarian) fragments
C25-E	520	75	10% calcareous micrite matrix, 90% foraminifera fragments
C25-F	593	2	88% calcareous micrite (15% organic, 85% coccolithic) matrix, 10% foraminifera fragments, 2% amorphous silica (radiolarian) fragments
	595		

Core 38SL

NOTE: Bent barrel, core #26 sat on deck for >1 hour, loss from both top and bottom of core

C26-A	6	144	83% calcareous micrite (15% organic, 85% coccolithic) matrix, 15% foraminifera fragments, 2% amorphous silica (radiolarian) fragments
C26-B	60	90	83% calcareous micrite (15% organic, 85% coccolithic) matrix, 15% foraminifera fragments, 2% amorphous silica (radiolarian) fragments
C26-C	148	2	85% calcareous micrite (10% organic, 90% coccolithic) matrix, 15% foraminifera fragments
	150		

Core 39SL

C27-A	20	573	90% calcareous micrite (25% organic, 75% coccolithic) matrix, 2% foraminifera fragments, 8% amorphous silica (radiolarian) fragments
C27-B	110	483	90% calcareous micrite (15% organic, 85% coccolithic) matrix, 5% foraminifera fragments, 5% amorphous silica (radiolarian) fragments
C27-C	285	308	90% calcareous micrite (15% organic, 85% coccolithic) matrix, 5% foraminifera fragments, 5% amorphous silica (radiolarian)

			fragments
C27-D	365	228	88% calcareous micrite (20% organic, 80% coccolithic) matrix, 10% foraminifera fragments, 2% amorphous silica (radiolarian) fragments
C27-E	460	133	85% calcareous micrite (10% organic, 90% coccolithic) matrix, 15% foraminifera fragments
C27-F	570	23	93% calcareous micrite (15% organic, 85% coccolithic) matrix, 5% foraminifera fragments, 2% amorphous silica (radiolarian) fragments
	593		

Core 40SL

C28-A	20	555	90% calcareous micrite (20% organic, 80% coccolithic) matrix, 8% foraminifera fragments, 2% amorphous silica (radiolarian) fragments
C28-B	120	455	88% calcareous micrite (25% organic, 75% coccolithic) matrix, 10% foraminifera fragments, 2% amorphous silica (radiolarian) fragments
C28-C	270	305	9% calcareous micrite matrix, 90% foraminifera fragments, 1% amorphous silica (radiolarian) fragments
C28-D	385	190	89% calcareous micrite (10% organic, 90% coccolithic) matrix, 10% foraminifera fragments, 1% amorphous silica (radiolarian) fragments
C28-E	490	85	83% calcareous micrite (15% organic, 85% coccolithic) matrix, 15% foraminifera fragments, 2% amorphous silica (radiolarian) fragments
C28-F	570	5	73% calcareous micrite (10% organic, 90% coccolithic) matrix, 25% foraminifera fragments, 2% amorphous silica (radiolarian) fragments
	575		

Core 44SL

C29-A	20	545	93% calcareous micrite (10% organic, 90% coccolithic) matrix, 5% foraminifera fragments, 2% amorphous silica (radiolarian) fragments
C29-B	160	405	93% calcareous micrite (10% organic, 90% coccolithic) matrix, 5% foraminifera fragments, 2% amorphous silica (radiolarian) fragments
C29-C	245	320	93% calcareous micrite (15% organic, 85% coccolithic) matrix, 5% foraminifera fragments, 2% amorphous silica (radiolarian) fragments
C29-D	315	250	88% organic-rich calcareous micrite matrix, 10% foraminifera fragments, 2% amorphous silica (radiolarian) fragments
C29-E	460	105	75% organic-rich calcareous micrite matrix, 20% foraminifera

			fragments, 5% amorphous silica (radiolarian) fragments
C29-F	560	5	70% calcareous micrite (30% organic, 70% coccolithic) matrix, 25% foraminifera fragments, 5% amorphous silica (radiolarian) fragments
	565		

Core 45SL

NOTE: Bent barrel, top portion of core #30 lost			
C30-A	20	490	83% calcareous micrite (15% organic, 85% coccolithic) matrix, 15% foraminifera fragments, 2% amorphous silica (radiolarian) fragments
C30-B	160	350	93% calcareous micrite (10% organic, 90% coccolithic) matrix, 5% foraminifera fragments, 2% amorphous silica (radiolarian) fragments
C30-C	275	235	93% calcareous micrite (20% organic, 80% coccolithic) matrix, 5% foraminifera fragments, 2% amorphous silica (radiolarian) fragments
C30-D	420	90	82% organic-rich calcareous micrite matrix, 10% foraminifera fragments, 8% amorphous silica (radiolarian) fragments
C30-E	508	2	75% calcareous micrite (30% organic, 70% coccolithic) matrix, 20% foraminifera fragments, 5% amorphous silica (radiolarian) fragments
	510		

Appendix 4: Pore water samples taken

Porewaters core 1 (1SL)

total length:		**476**				
sample	measured from bottom		measured from top		**depth**	**+/-**
ID	from	to	from	to	**cm**	**cm**
1	468	472	4	8	**6,0**	**2**
2	460	463	13	16	**14,5**	**1,5**
3	448	452	24	28	**26,0**	**2**
4	432	437	39	44	**41,5**	**2,5**
5	415	419	57	61	**59,0**	**2**
6	398	402	74	78	**76,0**	**2**
7	385	389	87	91	**89,0**	**2**
8	365	369	107	111	**109,0**	**2**
9	339	343	133	137	**135,0**	**2**
10	298	302	174	178	**176,0**	**2**
11	250	254	222	226	**224,0**	**2**
12	199	203	273	277	**275,0**	**2**
13	147	151	325	329	**327,0**	**2**
14	91	95	381	385	**383,0**	**2**
15	54	59	417	422	**419,5**	**2,5**
16	15	18	458	461	**459,5**	**1,5**

Porewaters core 2 (2SL)

total length:		**380**				
sample	measured from bottom		measured from top		**depth**	**+/-**
ID	from	to	from	to	**cm**	**cm**
1	343	347	33	37	**35,0**	**2**
2	334	338	42	46	**44,0**	**2**
3	310	313	67	70	**68,5**	**1,5**
4	294	298	82	86	**84,0**	**2**
5	279	283	97	101	**99,0**	**2**
6	262	265	115	118	**116,5**	**1,5**
7	239	243	137	141	**139,0**	**2**
8	183	186	194	197	**195,5**	**1,5**
9	160	164	216	220	**218,0**	**2**
10	137	143	237	243	**240,0**	**3**
11	106	110	270	274	**272,0**	**2**
12	71	75	305	309	**307,0**	**2**
13	37	43	337	343	**340,0**	**3**
14	13	16	364	367	**365,5**	**1,5**

Porewaters core 3 (3SL)

total length:		**510**				
sample	measured from bottom		measured from top		**depth**	**+/-**
ID	from	to	from	to	**cm**	**cm**
1	494	499	11	16	**13,5**	**2,5**
2	473	478	32	37	**34,5**	**2,5**
3	451	456	54	59	**56,5**	**2,5**
4	436	440	70	74	**72,0**	**2**
5	403	409	101	107	**104,0**	**3**
6	348	359	151	162	**156,5**	**5,5**
7	297	303	207	213	**210,0**	**3**
8	250	256	254	260	**257,0**	**3**
9	198	204	306	312	**309,0**	**3**
10	152	158	352	358	**355,0**	**3**
11	101	107	403	409	**406,0**	**3**

12	62	66	444	448	**446,0**	**2**
13	35	40	470	475	**472,5**	**2,5**
14	10	14	496	500	**498,0**	**2**

Porewaters core 4 (5SL)

total length:	**430**					
sample	measured from bottom		measured from top		**depth**	**+/-**
ID	from	to	from	to	**cm**	**cm**
1	415	420	10	15	**12,5**	**2,5**
2	404	410	20	26	**23,0**	**3**
3	394	400	30	36	**33,0**	**3**
4	362	370	60	68	**64,0**	**4**
5	347	354	76	83	**79,5**	**3,5**
6	332	339	91	98	**94,5**	**3,5**
7	295	303	127	135	**131,0**	**4**
8	248	255	175	182	**178,5**	**3,5**
9	197	204	226	233	**229,5**	**3,5**
10	147	153	277	283	**280,0**	**3**
11	99	105	325	331	**328,0**	**3**
12	59	71	359	371	**365,0**	**6**
13	34	38	392	396	**394,0**	**2**

Porewaters core 5 (6SL)

total length:	**190**					
sample	measured from bottom		measured from top		**depth**	**+/-**
ID	from	to	from	to	**cm**	**cm**
1	183	186	4	7	**5,5**	**1,5**
2	173	177	13	17	**15,0**	**2**
3	161	163	27	29	**28,0**	**1**
4	150	156	34	40	**37,0**	**3**
5	132	138	52	58	**55,0**	**3**
6	109	115	75	81	**78,0**	**3**
7	82	89	101	108	**104,5**	**3,5**
8	61	66	124	129	**126,5**	**2,5**
9	42	48	142	148	**145,0**	**3**
10	14	19	171	176	**173,5**	**2,5**

Porewaters core 6 (7SL)

total length:	**490**					
sample	measured from bottom		measured from top		**depth**	**+/-**
ID	from	to	from	to	**cm**	**cm**
1	493	498	2	7	**4,5**	**2,5**
2	481	485	15	19	**17,0**	**2**
3	466	472	28	34	**31,0**	**3**
4	453	458	42	47	**44,5**	**2,5**
5	414	418	82	86	**84,0**	**2**
6	390	395	105	110	**107,5**	**2,5**
7	365	370	130	135	**132,5**	**2,5**
8	327	333	167	173	**170,0**	**3**
9	275	285	215	225	**220,0**	**5**
10	230	236	264	270	**267,0**	**3**
11	177	184	316	323	**319,5**	**3,5**
12	127	133	367	373	**370,0**	**3**
13	77	83	417	423	**420,0**	**3**
14	28	38	462	472	**467,0**	**5**

Porewaters core 7 (8SL)

total length: **570**

sample	measured from bottom		measured from top		depth	+/-
ID	from	to	from	to	cm	cm
1	564	568	2	6	4,0	2
2	554	558	12	16	14,0	2
3	540	544	26	30	28,0	2
4	510	515	55	60	57,5	2,5
5	498	503	67	72	69,5	2,5
6	463	468	102	107	104,5	2,5
7	413	419	151	157	154,0	3
8	365	371	199	205	202,0	3
9	302	308	262	268	265,0	3
10	262	267	303	308	305,5	2,5
11	208	214	356	362	359,0	3
12	160	165	405	410	407,5	2,5
13	101	105	465	469	467,0	2
14	57	62	508	513	510,5	2,5
15	21	25	545	549	547,0	2

Porewaters core 8 (10SL)

total length: 460

sample	measured from bottom		measured from top		depth	+/-
ID	from	to	from	to	cm	cm
1	452	458	2	8	5,0	3
2	434	438	22	26	24,0	2
3	404	408	52	56	54,0	2
4	368	372	88	92	90,0	2
5	328	332	128	132	130,0	2
6	298	302	158	162	160,0	2
7	264	278	182	196	189,0	7
8	197	203	257	263	260,0	3
9	151	155	305	309	307,0	2
10	104	110	350	356	353,0	3
11	50	55	405	410	407,5	2,5
12	16	21	439	444	441,5	2,5

Porewaters core 9 (11SL)

total length: 575

sample	measured from bottom		measured from top		depth	+/-
ID	from	to	from	to	cm	cm
1	560	563	12	15	13,5	1,5
2	544	547	28	31	29,5	1,5
3	522	526	49	53	51,0	2
4	494	498	77	81	79,0	2
5	468	473	102	107	104,5	2,5
6	418	424	151	157	154,0	3
7	347	354	221	228	224,5	3,5
8	275	281	294	300	297,0	3
9	156	162	413	419	416,0	3
10	109	114	461	466	463,5	2,5
11	59	65	510	516	513,0	3
12	21	27	548	554	551,0	3

Porewaters core 10 (11SL)

total length: 575

sample	measured from bottom		measured from top		depth	+/-
ID	from	to	from	to	cm	cm
1	565	571	4	10	7,0	3
2	553	558	17	22	19,5	2,5

3	513	518	57	62	**59,5**	**2,5**
4	471	476	99	104	**101,5**	**2,5**
5	427	433	142	148	**145,0**	**3**
6	370	375	200	205	**202,5**	**2,5**
7	324	330	245	251	**248,0**	**3**
8	264	269	306	311	**308,5**	**2,5**
9	171	177	398	404	**401,0**	**3**
10	120	125	450	455	**452,5**	**2,5**
11	69	75	500	506	**503,0**	**3**
12	26	31	544	549	**546,5**	**2,5**

Porewaters core 11 (14SL)

total length: 547

sample	measured from bottom		measured from top		**depth**	**+/-**
ID	from	to	from	to	**cm**	**cm**
1	536	541	6	11	**8,5**	**2,5**
2	522	527	20	25	**22,5**	**2,5**
3	507	512	35	40	**37,5**	**2,5**
4	458	463	84	89	**86,5**	**2,5**
5	422	426	121	125	**123,0**	**2**
6	371	376	171	176	**173,5**	**2,5**
7	306	310	237	241	**239,0**	**2**
8	227	233	314	320	**317,0**	**3**
9	179	183	364	368	**366,0**	**2**
10	128	134	413	419	**416,0**	**3**
11	56	60	487	491	**489,0**	**2**
12	33	36	511	514	**512,5**	**1,5**

Porewaters core 12 (15SL)

total length: 430

sample	measured from bottom		measured from top		**depth**	**+/-**
ID	from	to	from	to	**cm**	**cm**
1	424	428	2	6	**4,0**	**2**
2	409	413	17	21	**19,0**	**2**
3	393	398	32	37	**34,5**	**2,5**
4	364	369	61	66	**63,5**	**2,5**
5	345	350	80	85	**82,5**	**2,5**
6	308	315	115	122	**118,5**	**3,5**
7	262	268	162	168	**165,0**	**3**
8	208	214	216	222	**219,0**	**3**
9	157	162	268	273	**270,5**	**2,5**
10	102	107	323	328	**325,5**	**2,5**
11	60	65	365	370	**367,5**	**2,5**
12	23	27	403	407	**405,0**	**2**

Porewaters core 13 (16SL)

total length: 275

sample	measured from bottom		measured from top		**depth**	**+/-**
ID	from	to	from	to	**cm**	**cm**
1	265	270	5	10	**7,5**	**2,5**
2	235	240	35	40	**37,5**	**2,5**
3	191	196	79	84	**81,5**	**2,5**
4	158	164	111	117	**114,0**	**3**
5	105	110	165	170	**167,5**	**2,5**
6	70	76	199	205	**202,0**	**3**
7	43	48	227	232	**229,5**	**2,5**
8	17	23	252	258	**255,0**	**3**

Porewaters core 14 (17SL)

total length:		365				
sample	measured from bottom		measured from top		depth	+/-
ID	from	to	from	to	cm	cm
1	358	363	2	7	4,5	2,5
2	343	349	16	22	19,0	3
3	265	271	94	100	97,0	3
4	221	227	138	144	141,0	3
5	177	182	183	188	185,5	2,5
6	123	129	236	242	239,0	3
7	65	71	294	300	297,0	3
8	24	28	337	341	339,0	2

Porewaters core 15 (23SL)

total length:		394				
sample	measured from bottom		measured from top		depth	+/-
ID	from	to	from	to	cm	cm
1	383	389	5	11	8,0	3
2	369	375	19	25	22,0	3
3	337	343	51	57	54,0	3
4	305	312	82	89	85,5	3,5
5	247	254	140	147	143,5	3,5
6	150	155	239	244	241,5	2,5
7	92	98	296	302	299,0	3
8	17	24	370	377	373,5	3,5

Porewaters core 16 (24SL)

total length:		406				
sample	measured from bottom		measured from top		depth	+/-
ID	from	to	from	to	cm	cm
1	396	403	3	10	6,5	3,5
2	377	382	24	29	26,5	2,5
3	337	344	62	69	65,5	3,5
4	310	316	90	96	93,0	3
5	264	269	137	142	139,5	2,5
6	167	174	232	239	235,5	3,5
7	59	65	341	347	344,0	3
8	20	26	380	386	383,0	3

Porewaters core 17 (25SL)

total length:		382				
sample	measured from bottom		measured from top		depth	+/-
ID	from	to	from	to	cm	cm
1	376	381	1	6	3,5	2,5
2	359	367	15	23	19,0	4
3	328	335	47	54	50,5	3,5
4	284	291	91	98	94,5	3,5
5	231	236	146	151	148,5	2,5
6	154	160	222	228	225,0	3
7	101	106	276	281	278,5	2,5
8	8	12	370	374	372,0	2

Porewaters core 18 (26SL)

total length:		468				
sample	measured from bottom		measured from top		depth	+/-
ID	from	to	from	to	cm	cm
1	460	465	3	8	5,5	2,5

2	448	454	14	20	**17,0**	**3**
3	412	420	48	56	**52,0**	**4**
4	374	381	87	94	**90,5**	**3,5**
5	324	330	138	144	**141,0**	**3**
6	285	291	177	183	**180,0**	**3**
7	228	234	234	240	**237,0**	**3**
8	134	141	327	334	**330,5**	**3,5**
9	61	66	402	407	**404,5**	**2,5**
10	21	26	442	447	**444,5**	**2,5**

Porewaters core 19 (27SL)

total length: 328

sample	measured from bottom		measured from top		**depth**	**+/-**
ID	from	to	from	to	**cm**	**cm**
1	314	320	8	14	**11,0**	**3**
2	299	304	24	29	**26,5**	**2,5**
3	271	276	52	57	**54,5**	**2,5**
4	225	230	98	103	**100,5**	**2,5**
5	182	187	141	146	**143,5**	**2,5**
6	114	119	209	214	**211,5**	**2,5**
7	88	94	234	240	**237,0**	**3**
8	25	32	296	303	**299,5**	**3,5**

Porewaters core 20 (30SL)

total length: 575

sample	measured from bottom		measured from top		**depth**	**+/-**
ID	from	to	from	to	**cm**	**cm**
1	568	573	2	7	**4,5**	**2,5**
2	553	559	16	22	**19,0**	**3**
3	533	540	35	42	**38,5**	**3,5**
4	490	495	80	85	**82,5**	**2,5**
5	430	435	140	145	**142,5**	**2,5**
6	386	391	184	189	**186,5**	**2,5**
7	324	329	246	251	**248,5**	**2,5**
8	250	255	320	325	**322,5**	**2,5**
9	157	163	412	418	**415,0**	**3**
10	126	132	443	449	**446,0**	**3**
11	52	57	518	523	**520,5**	**2,5**
12	18	25	550	557	**553,5**	**3,5**

Porewaters core 21 (31SL)

total length: 575

sample	measured from bottom		measured from top		**depth**	**+/-**
ID	from	to	from	to	**cm**	**cm**
1	566	571	4	9	**6,5**	**2,5**
2	549	556	19	26	**22,5**	**3,5**
3	529	534	41	46	**43,5**	**2,5**
4	482	487	88	93	**90,5**	**2,5**
5	432	437	138	143	**140,5**	**2,5**
6	383	388	187	192	**189,5**	**2,5**
7	315	320	255	260	**257,5**	**2,5**
8	250	255	320	325	**322,5**	**2,5**
9	188	193	382	387	**384,5**	**2,5**
10	123	128	447	452	**449,5**	**2,5**
11	75	80	495	500	**497,5**	**2,5**
12	20	25	550	555	**552,5**	**2,5**

Porewaters core 22 (32SL)

total length: 575

sample	measured from bottom		measured from top		depth	+/-
ID	from	to	from	to	cm	cm
1	568	573	2	7	**4,5**	**2,5**
2	557	562	13	18	**15,5**	**2,5**
3	536	541	34	39	**36,5**	**2,5**
4	482	487	88	93	**90,5**	**2,5**
5	431	436	139	144	**141,5**	**2,5**
6	381	386	189	194	**191,5**	**2,5**
7	316	321	254	259	**256,5**	**2,5**
8	250	255	320	325	**322,5**	**2,5**
9	173	178	397	402	**399,5**	**2,5**
10	112	117	458	463	**460,5**	**2,5**
11	74	79	496	501	**498,5**	**2,5**
12	18	23	552	557	**554,5**	**2,5**

Porewaters core 23 (33SL)

total length: 575

sample	measured from bottom		measured from top		depth	+/-
ID	from	to	from	to	cm	cm
1	566	571	4	9	**6,5**	**2,5**
2	545	549	26	30	**28,0**	**2**
3	526	531	44	49	**46,5**	**2,5**
4	466	471	104	109	**106,5**	**2,5**
5	408	413	162	167	**164,5**	**2,5**
6	365	370	205	210	**207,5**	**2,5**
7	309	314	261	266	**263,5**	**2,5**
8	223	228	347	352	**349,5**	**2,5**
9	154	159	416	421	**418,5**	**2,5**
10	110	115	460	465	**462,5**	**2,5**
11	59	64	511	516	**513,5**	**2,5**
12	18	23	552	557	**554,5**	**2,5**

Porewaters core 24 (34SL)

total length: 575

sample	measured from bottom		measured from top		depth	+/-
ID	from	to	from	to	cm	cm
1	570	575	0	5	**2,5**	**2,5**
2	558	563	12	17	**14,5**	**2,5**
3	530	535	40	45	**42,5**	**2,5**
4	487	492	83	88	**85,5**	**2,5**
5	439	444	131	136	**133,5**	**2,5**
6	386	391	184	189	**186,5**	**2,5**
7	316	321	254	259	**256,5**	**2,5**
8	254	259	316	321	**318,5**	**2,5**
9	185	190	385	390	**387,5**	**2,5**
10	110	115	460	465	**462,5**	**2,5**
11	70	75	500	505	**502,5**	**2,5**
12	27	32	543	548	**545,5**	**2,5**

Porewaters core 25 (37SL)

total length: 574

sample	measured from bottom		measured from top		depth	+/-
ID	from	to	from	to	cm	cm
1	566	571	3	8	**5,5**	**2,5**
2	546	551	23	28	**25,5**	**2,5**
3	520	525	49	54	**51,5**	**2,5**
4	453	458	116	121	**118,5**	**2,5**
5	407	412	162	167	**164,5**	**2,5**

6	369	374	200	205	**202,5**	**2,5**
7	310	315	259	264	**261,5**	**2,5**
8	238	243	331	336	**333,5**	**2,5**
9	158	163	411	416	**413,5**	**2,5**
10	111	116	458	463	**460,5**	**2,5**
11	59	64	510	515	**512,5**	**2,5**
12	19	24	550	555	**552,5**	**2,5**

Porewaters core 26 (38SL)

total length: 150

sample	measured from bottom		measured from top		**depth**	**+/-**
ID	from	to	from	to	**cm**	**cm**
1	117	122	28	33	**30,5**	**2,5**
2	90	95	55	60	**57,5**	**2,5**
3	76	81	69	74	**71,5**	**2,5**
4	57	62	88	93	**90,5**	**2,5**
5	31	36	114	119	**116,5**	**2,5**
6	4	9	141	146	**143,5**	**2,5**

Porewaters core 27 (39SL)

total length: 575

sample	measured from bottom		measured from top		**depth**	**+/-**
ID	from	to	from	to	**cm**	**cm**
1	566	570	5	9	**7,0**	**2**
2	549	554	21	26	**23,5**	**2,5**
3	520	526	49	55	**52,0**	**3**
4	508	514	61	67	**64,0**	**3**
5	459	464	111	116	**113,5**	**2,5**
6	366	373	202	209	**205,5**	**3,5**
7	283	290	285	292	**288,5**	**3,5**
8	210	215	360	365	**362,5**	**2,5**
9	154	159	416	421	**418,5**	**2,5**
10	105	110	465	470	**467,5**	**2,5**
11	55	60	515	520	**517,5**	**2,5**
12	18	23	552	557	**554,5**	**2,5**

Porewaters core 28 (40SL)

total length: 575

sample	measured from bottom		measured from top		**depth**	**+/-**
ID	from	to	from	to	**cm**	**cm**
1	545	550	25	30	**27,5**	**2,5**
2	534	539	36	41	**38,5**	**2,5**
3	513	515	60	62	**61,0**	**1**
4	494	499	76	81	**78,5**	**2,5**
5	440	445	130	135	**132,5**	**2,5**
6	386	391	184	189	**186,5**	**2,5**
7	303	308	267	272	**269,5**	**2,5**
8	238	243	332	337	**334,5**	**2,5**
9	179	184	391	396	**393,5**	**2,5**
10	116	121	454	459	**456,5**	**2,5**
11	47	52	523	528	**525,5**	**2,5**
12	18	23	552	557	**554,5**	**2,5**

Porewaters core 29 (44SL)

total length: 565

sample	measured from bottom		measured from top		**depth**	**+/-**
ID	from	to	from	to	**cm**	**cm**
1	547	553	12	18	**15,0**	**3**

2	522	527	38	43	**40,5**	**2,5**
3	508	515	50	57	**53,5**	**3,5**
4	495	500	65	70	**67,5**	**2,5**
5	456	463	102	109	**105,5**	**3,5**
6	407	415	150	158	**154,0**	**4**
7	339	346	219	226	**222,5**	**3,5**
8	240	247	318	325	**321,5**	**3,5**
9	159	167	398	406	**402,0**	**4**
10	109	115	450	456	**453,0**	**3**
11	62	67	498	503	**500,5**	**2,5**
12	19	24	541	546	**543,5**	**2,5**

Porewaters core 30 ("Bendy Bob") (45SL)

total length: 510

sample	measured from bottom		measured from top		**depth**	**+/-**
ID	from	to	from	to	**cm**	**cm**
1	497	502	8	13	**10,5**	**2,5**
2	457	463	47	53	**50,0**	**3**
3	406	412	98	104	**101,0**	**3**
4	355	362	148	155	**151,5**	**3,5**
5	273	279	231	237	**234,0**	**3**
6	160	166	344	350	**347,0**	**3**
7	108	114	396	402	**399,0**	**3**
8	56	63	447	454	**450,5**	**3,5**

Appendix 5: Core Descriptions

CORE 1

NB core descriptions only given where porosity samples taken

Section	Depth cmbsf	Pore Water	Porosity	Smear Slide	General Description
S17 0-115	0	#1 (6.0)	#1 (10)	P (6)	Least stiff, med. brown with mottling, many forams
		#2 (14.5)	#2 (18)	O (16)	Mottled horizon: fudge and med. brown
	20			N (26)	
		#3 (26.0)	#3 (31)		
	40	#4 (41.5)	#4 (37)	M (41)	Fudge brown, with some med. brown bioturbation
		#5 (59.0)	#5 (63)		
	60			L (61)	
		#6 (76.0)	#6 (79.5)		
	80				General lightening trend
		#7 (89.0)	#7 (92.5)		
	100	#8 (109.0)	#8 (112.5)	I (111)	
S16 115-123					
	120				
S15 123-146		#9 (135.0)	#9 (139.5	H (136)	Little white forams evident
	140				
S14 156-146					
	160				
		#10 (176.0)	#10 (182.5)	G (176)	Less stiff, with fine layers of foram sand
S13 196-156	180				
S12 206-196	200				
	220	#11 (224.0)	#11 (228.5)	F (226)	Dark fudge brownie matrix
S11 246-206					
	240				
S10 256-246		#12 (275.0)	#12 (279.5)		
	260				
				E (276)	Darker, still stiff, highly bioturbated
S9 296-256	280				
S8 306-296	300				
S 7 346-306	320	#13 (327.0)	#13 (331.5)	D (326)	
					More frequent bioturbation
	340				
S6 356-346					
	360				
S5 396-356					
	380	#14 (383.0)	#14 (387.5)	C (381)	brown bioturbation
S4 406 - 396	400				
		#15 (419.5)	#15 (423)		
	420			B (421)	More of the same, with bioturbation
S3 446 - 406)					
	440				
		#16 (459.5)	#16 (454) 16 ml		
S2 456-446	460			A (461)	Khaki- tan, stiff fine mud
S1 476-456)	476				

CORE 2

Section	Depth cmbsf	Pore Water	Porosity	Smear Slide	General Description
	0			J (5)	
				I (15)	Getting very soupy. Top 35cm may be repeated
S9	20				
0-50		#1 (35.0)	#1 (39)		
	40			H (40)	Wetter, lighter brown
		#2 (44.0)	#2 (49)		Mottled darker and lighter brown, many forams
S8 50-60	60				Lighter brown, wetter
		#3 (68.5)	#3 (72)	G (70)	
	80	#4 (84.0)	#4 (88)		
	100	#5 (99.0)	#5 (103)		
S7		#6 (116.5)	#6 (120	F (110)	Darker brown, with dark/lighter dark brown mottling
60-150	120				
					Grading to darker brown matrix
	140	#7 (139.0)	#7 (143)		
S6 150-160	160			E (165)	Chocolate brown, with prominent white forams
	180				Transition from dark tan to chocolate brown
		#8 (195.5)	#8 (200)		
	200				
S5				D (210)	
160-250	220	#9 (218.0)	#9 (222)		
	240	#10 (240.0)	#10 (245)	C (240)	
S4 250-260	260				
		#11 (272.0)	#11 (277)		
	280				Increasingly bioturbated
	300				
S3 260-350		#12 (307.0)	#12 (311)	B (310)	
	320				
	340	#13 (340.0)	#13 (345)	A (335)	
S2 350-360	360				
		#14 (365.5)	#14 (369)		
S1 360-380	380				Tan-khaki, very stiff, fine mud, with some smudges of bioturbation

CORE 3

Section	Depth cmbsf	Pore Water	Porosity	Smear Slide	General Description
	0				Dark chocolate brown matrix. Consistency = less
		#1 (13.5)	#1 (19)	J (5)	stiff , 'soupy'. Possible 0.5m lost from top of core.
	20				Medium chocolate brown matrix. Gradational change to.......
		#2 (35.5)	#2 (39)	I (25)	Light chocolate brown matrix. Gradational change to.....
S21 (40)	40				
S20 (50)		#3 (56.5)	#3 (59)	H (55)	Light & Medium chocolate brown mottled matrix. Fewer forams.
	60				
		#4 (72.0)	#4 (76)		
S19 (80)	80				
S18 (90)					Light Medium chocolate brown matrix.More forams.
	100				
		#5 (104.0)	#5 (108)	G (110)	
	120				
S17 (130)					
S16 (140)	140				
		#6 (156.5)			Medium chocolate brown matrix. Stiff, fine mud. Foram rich.
	160				
			#6 (162)		
S15 (180)	180				
S14 (190)					Medium chocolate brown matrix.
	200				
		#7 (210.0)	#7 (214)	F (210)	Gradual darkening of matrix. Remains stiff. Fewer forams.
	220				
S13 (230)					Light chocolate brown maxtrix. Stiff, fine mud. Foram rich.
S12 (240)	240				
		#8 (257.0)			
	260				Gradational lightening of matrix
			#8 (261)		
S11 (280)	280				
S10 (290)					
	300				
		#9 (309.0)	#9 (313)	E (310)	10-20cm transition from 'soupy' dark chocolate brown
	320				to stiffer light chocolate brown matrix.
S9 (330)					Dark chocolate brown matrix. 'Soupy'.
S8 (340)	340				forams increase.
		#10 (355.0)		D (350)	
	360		#10 (360)		
S7 (380)	380				forams become evident
S6 (390)					Transition in matrix to darker chocolate brown (gradational)
	400			C (400)	Fudge consistency.(bioturb. mottling dk. & medium brown)
		#11 (406.0)	#11 (411)		
	420				abrupt transition in matrix from tan to medium brown
S5 (430)					
S4 (440)	440			B (440)	
		#12 (446.0)	#12 (450)		
	460				increasing bioturbation, transition from white to
		#13 (472.5)	#13 (478)		brown smudges
S3 (480)	480				
S2 (490)					

500 #14 (498.0) A (500)

S1 (510) 510

Tan-Khaki Matrix. Very stiff consistency. Fine mud.
White biouturbation smudges.

CORE 4

Section	Depth cmbsf	Pore Water	Porosity	Smear Slide	General Description
	0			H (0)	Lightening to top. Foram soup
		#1 (12.5)			
	20	#2 (23.0)	#2 (17)		
S17		#3 (33.0)	#3 (38)	G (30)	
	40				Lightening
					Becoming sandier
S16	60	#4 (64.0)	#4 (61)		
S15	80	#5 (79.5)	#5 (77)		Medium tan-khaki
		#6 (94.5)	#6 (91)	F (90)	
	100				Lightening trend
S14					
	120				
		#7 (131.0)	#7 (137)	E (130)	Transition back to darker tan
S13	140				
					Transition to lighter brown- tan/khaki matrix
S12	160				
	180	#8 (178.5)	#8 (184)		
S11					
	200				
S10					
	220	#9 (229.5)	#9 (233)		
S9					
	240			D (245)	Zone of dark brown bioturbation
S8	260				
				C (270)	
S7	280	#10 (280.0)	#10 (283)		
	300				
S6					
	320				Increasing bioturbation
S5		#11 (328.0)	#11 (333)		
	340				
S4	360	#12 (365.0)	#12 (372)		
S3	380				
		#13 (394.0)	#13 (398)	B (390)	
	400				
S2					
	420			A (426)	
S1	430				Foram rich grey-brown fine mud with some patchy bioturbation, stiff.

CORE 5

Section	Depth cmbsf	Pore Water	Porosity	Smear Slide	General Description
	0	#1 (5.5)		E (5)	
		#2 (15.0)	#2 (12)		
S8 0-30	20				Transition- slightly lighter and less bioturbated
		#3 (28.0)	#3 (19)	D (35)	
	40	#4 (37.0)	#4 (40)		
S7 30-60		#5 (55.0)	#5 (58)		
	60			C (65)	
S6 60-70		#6 (78.0)	#6 (84)		Starting to get stiff
	80				
S5 70-110	100	#7 (104.5)	#7 (108)		
				B (115)	
S4 110-120	120	#8 (126.5)	#8 (131)		
	140	#9 (145.0)	#9 (150)		
S3 120-160					
	160				
S2 160-170		#10 (173.5)	#10 (178)		
	180			A (185)	Foram rich, tan-khaki, stiff fine mud, bioturbated
S1 170-190	190				Approximate pre-oozing core length

CORE 6

Section	Depth cmbsf	Pore Water	Porosity	Smear Slide	General Description
	0				Tan matrix. Fine mud. 'Soupy' consistency. Foram rich.
		#1 (4.5)	#1 (9)	F (0)	
	20	#2 (17.0)	#2 (19)		
		#3 (31.0)	#3 (32)		Abrupt transition in matrix consistency from stiff &
	40				bioturbated to 'soupy'
S20		#4 (44.0)	#4 (48)		
S19	60				
			#5 (77)		
	80				
S18		#5 (84.0)			
S17	100		#6 (113)		
		#6 (107.5)		E (105)	
	120				
		#7 (132.5)	#7 (137)		
S16	140				
S15					
	160				Matrix consistency V. Stiff.
		#8 (170.0)	#8 (173)		
	180				
S14					
S13	200				
				D (210)	
	220				
		#9 (220.0)	#9 (225)		
S12	240				Gradational change in matrix consistency, becoming less
S11					stiff with increased bioturbation.
	260				
		#10 (267.0)	#10 (272)		
	280				
S10				C (280)	295-310:
S9	300				Zone containing fragments of altered (palagonite) glass,
		#11 (319.0)	#11 (325)		green/brown, angular. Up to 12mm dimensions.
	320				
S8	340				
S7					
	360				
		#12 (370.0)	#12 (376)	B (360)	
	380				Matrix remains constant. Little change in composition.
S6					
S5	400				
	420				
		#13 (420.0)	#13 (424)		
S4	440				
S3					
	460				
		#14 (467.0)	#14 (470)	A (468)	
S2	480				
S1	490				Stiff, fine tan-khaki mud. Patchy bioturbation. Foram rich.

CORE 7

Section	Depth cmbsf	Pore Water	Porosity	Smear Slide	General Description
	0	#1 (4)	#1 (9)	L (1)	Medium brown
		#2 (14)	#2 (19)		
	20				Lightening
S23 0-40		#3 (28)	#3 (34)		
	40				
S22 40-50					Medium to dark brown mud with big forams
	60	#4 (57.5)	#4 (64)		
		#5 (69.5)	#5 (74)		
S21 50-90	80			K (83)	Grading to fine mud
				J (90)	
S20 90-100	100	#6 (104.5)	#6 (110)	I (98)	Sharp transition med. brown stiff to tan-khaki foram rich mud
				H (105)	
S19 100-130	120			G (120)	Another mottled transition
S18 130-140	140				Mottled transition
		#7 (154.0)	#7 (159)		Lightening
	160				
S17 140-180					Transition from tan to light brown mud
	180				
S16 180-190					Lightening
	200	#8 (202.0)	#8 (207)		
					Light-med. brown fine mud, stiff with occasional forams
S15 190-230	220			F (220)	Increase in mud content
S14 230-240	240				
					Sharp change to well sorted foram grains in med. to coase matrix
	260	#9 (265.0)	#9 (270)	E (262)	Mottled change to dark brown
S13 240-280				D (275)	
	280				Still fine mud, bioturbated
S12 280-290					
	300	#10 (305.5)	#10 (309)		
					Sharp transition form med. brown to light-med. matrix
S11 290-330	320				
					Lightening
S10 330-340	340				
					Darker- chocolate brown
	360	#11 (359.0)	#11 (362)		
S9 340-380					
	380				
S8 380-390					
	400				Lighter matrix
		#12 (407.5)	#12 (411)	C (415)	
S7 390-430	420				
S6 430-440	440				
					Gradual darkening
	460				
S5 440-480		#13 (467.0)	#13 (470)		
	480			B (480)	
S4 480-490					Darker zone, occasional forams

	500			
		#14 (510.5)	#14 (514)	Light- med. brown fine mud
S3 490-530	520			
				Darker zone
S2 530-540	540			
		#15 (547.0)	#15 (552)	
S1	560			
540-570	570			A (568) Light-med brown fine mud, some patchy bioturbation

CORE 8

Section	Depth cmbsf	Pore Water	Porosity	Smear Slide	General Description
	0	#1 (5.0)	#1 (6)	E (5)	
	20	#2 (24.0)	#2 (30)		
S5 0-60	40				
		#3 (54.0)	#3 (60)		
	60				
	80				Light but gritty, foram rich.
		#4 (90.0)	#4 (99)		
	100			D (105)	
S4	120				
60-160		#5 (130.0)	#5 (141)		
	140				
	160	#6 (160.0)	#6 (162)		
	180				
		#7 (189.0)	#7 (198)		
	200				Lightening back to light chocolate colour
S3	220				
160-260					
	240				
	260	#8 (260.0)	#8 (265)	C (265)	Darker, grittier, less forams
	280				
	300				Smoother texture with more forams
		#9 (307.0)	#9 (313)		
	320				
S2					
260-360	340				
		#10 (353.0)	#10 (360)	B (355)	
	360				
	380				
S1					
	400				
360-460		#11 (407.0)	#11 (412)		Some bioturbation smudges
	420				
	440	#12 (441.5)	#12 (453)		
				A (453)	
	460				Light chocolate coloured fine mud with gritty texture, foram rich, soupy

CORE 9

Section	Depth cmbsf	Pore Water	Porosity	Smear Slide	General Description
	0			F (5)	Lighter chocolate brown fine mud, stiff, foram rich
		#1(13.5)	#1 (16)		
S19 0-35	20				
		#2 (29.5)	#2 (34)		
S18 35-45	40				
		#3 (51.0)	#3 (54)		Slightly darker
S17	60				
45-85					
	80	#4 (79.0)	#4 (74)		
S16 85-95					
	100	#5 (104.5)	#5 (109)	E (95)	Wetter?
S15 95-125					
	120				
S14 125-135					
	140				
S13 135-175		#6 (154.0)	#6 (159)		
	160				
S12 175-185	180				
	200				Slightly darker
				D (215)	
	220	#7 (224.5)	#7 (229)		
S11					
185-275	240				
					Slightly lighter
	260				
S10 275-285	280				
	300	#8 (297.0)	#8 (300)		
	320				
				C (335)	
S9	340				
285-385					
	360				
	380				
S8 385-395					
	400				
S7		#9 416.0)	#9 (420)		
395-435	420				
S6 435-445	440				
				B (455)	
S5	460	#10 (463.5)	#10 (468)		
445-485					Less stiff
	480				
S4 485-495					

	500				
S3		#11 (513.0)	#11 (528)		
495-535	520				Med. chocolate brown
S2 535-545	540				
		#12 (551.0)	#12 (555)		Lightening, bioturbation smudges
S1	560			A (560)	
545-575	575				Stiff dark brown mud, sand sized forams

CORE 10

Section	Depth cmbsf	Pore Water	Porosity	Smear Slide	General Description
	0				Top much lighter, foram rich
		#1 (7.0)	#1 (5)	F (0)	
	20	#2 (19.5)	#2 (17)		
					Dark zone
	40				
	60	#3 (59.5)	#3 (59)		
S16 (80)	80				
				E (90)	
	100		#4 (99)		
		#4 (101.5)			Dark zone
S15 (120)	120				
S14 (130)				D (130)	
	140				
		#5 (145.0)	#5 (143)		
	160				
S13 (170)					
S12 (180)	180				~20cm thick dark zone
	200				
		#6 (202.5)	#6 (200)		
	220				
	240				
		#7 (248.0)	#7 (246)		
	260				
S11 (270)					
S10 (280)	280				
	300				Gradual lightening in colour
		#8 (308.5)	#8 (313)		
	320				
				C (330)	
	340				
S9 (360)	360				
S8 (370)					
	380				
	400				
		#9 (401.0)	#9 (400)		
S7 (420)	420				
S6 (430)					
	440				
		#10 (452.5)	#10 (451)	B (450)	
	460				
S5 (470)					Lighter chocolate brown, more forams
S4 (480)	480				

	500				
		#11 (503.0)	#11 (504)		
S3 (520)	520				Lightening in colour and increasing in bioturbation
S2 (530)					
	540				
		#12 (546.5)	#12 (546)	A (555)	
	560				
S1 (570)	570				Stiff, medium brown, some forams, not much bioturbation

CORE 11

Section	Depth cmbsf	Pore Water	Porosity	Smear Slide	General Description
	0			F (0)	
		#1 (8.5)			
	20				Slightly darker zone
		#2 (22.5)	#2 (24)		
	40	#3 (37.5)			
S17 (47)			#3 (43)		
S16 (57)	60				
	80				
		#4 (86.5)	#4 (92)		
S15 (97)	100				
S14 (107)					
	120				
		#5 (123.0)	#5 (127)		
	140				
S13 (147)					
S12 (157)	160			E (160)	
		#6 (173.5)	#6 (179)		
	180				Darker zone, less forams, much left stiff
	200				
	220				
		#7 (239.0)	#7 (244)		
	240				Chocolate
S11 (247)					
S10 (257)	260			D (260)	
	280				
	300				
		#8 (317.0)	#8 (323)		
	320				
					Slightly darker zone
	340				
S9 (347)					
S8 (357)	360				
		#9 (366.0)	#9 (371)		
	380			C (380)	Mottled change from darker to chocolate brown sandy, stiff and dry texture
S7 (397)	400				
S6 (407)		#10 (416.0)	#10 (419)		Darkening
	420				
					Slight darkening and stiffening
	440				
S5 (447)					
S4 (457)	460			B (460)	
	480				
		#11 (489.0)	#11 (494)		

S3 (497)	500				Brown and orange smudges of bioturbation (but not much)
S2 (507)		#12 (512.5)	#12 (517)		
	520			A (520)	
	540				
S1 (547)	547				Dark brown, stiff, dry, forams, no bioturbation

CORE 12

Section	Depth cmbsf	Pore Water	Porosity	Smear Slide	General Description
	0				Light chocolate, foram rich
		#1 (4)	#1 (11)	F (5)	
	20	#2 (19)			
		#3 (34.5)	#3 (29)		
S17 (40)	40				
S16 (50)					
	60				
		#4 (63.5)	#4 (67)		Increasing soupiness
	80				
S15 (90)		#5 (82.5)	#5 (87)		
S14 (100)	100				
		#6 (118.5)			
	120				
			#6 (125)	E (125)	
S13 (140)	140				
S12 (150)					Light chocolate, foram rich
	160			D (160)	
		#7 (165.0)	#7 (170)		Dark chocolate zone, muddy, less forams, less stiff.
	180				
S11 (190)					
S10 (200)	200				
		#8 (219.0)	#8 (222)		
	220				
				C (225)	Increasing forams, sandier
S9 (240)	240				
S8 (250)					
	260				
		#9 (270.5)	#9 (276)		
	280				Light chocolate
S7 (290)					
S6 (300)	300				
	320				
		#10 (325.5)	#10 (329)	B (325)	Med. chocolate, less stiff
S5 (340)	340				
S4 (350)					Lightening
	360				Mottled contact to dark chocolate, less stiff
		#11 (367.5)	#11 (374)		Mottled contact to med. chocolate, fairly stiff
	380				
S3 (390)					Stiffening
S2 (400)	400			A (400)	
		#12 (405.0)	#12 (409)		Cobble siyed chunk of glassy basalt, 18-22 above cc.
	420				
S1 (430)	430				Dark chocolate mud, not very stiff, some forams

CORE 13

Section	Depth cmbsf	Pore Water	Porosity	Smear Slide	General Description
	0				
		#1 (7.5)			
	20		#1 (14)		
				D (30)	
	40	#2 (37.5)			
			#2 (44)		
	60				Increasing soupiness
	80	#3 (81.5)			
S8 (95)			#3 (86)		
	100				
		#4 (114.0)		C (110)	
	120		#4 (122)		(Coarse and sized glass fragments)
S7 (135)					
S6 (145)	140				
					Transition to slightly lighter colour
	160				
		#5 (167.5)	#5 (171)	B (170)	Transition to slightly darker colour
S5 (185)	180				
S4 (195)					
	200	#6 (202.0)	#6 (206)		Increasing soupiness
	220				
S3 (235)		#7 (229.5)	#7 (233)		Mottled transition to med. brown
S2 (245)	240				
				A (250)	
	260	#8 (255.0)	#8 (258)		
S1 (275)	275				Medium-dark mottled, foram rich, not very stiff

CORE 14

Section	Depth cmbsf	Pore Water	Porosity	Smear Slide	General Description
	0	#1 (4.5)	#1 (10)	E (5)	Medium chocolate
S13 0-65	20	#2 (19.0)	#2 (25)		Slightly darker
	40				
	60				
S12 65-75	80			D (85)	Med. chocolate
S11 75-115	100	#3 (97.0)	#3 (101)		
	120				
S10 115-125					
	140	#4 (141.0)	#4 (147)	C (145)	
S9 125-165					Dark brown
	160				
S8 165-175	180	#5 (185.5)	#5 (191)		
S7 175-215	200				
					Med. chocolate
	220				
S6 215-225					
	240	#6 (239.0)	#6 (245)	B (245)	
S5 225-265					
	260				Real stiff, dark brown
S4 265-275					
	280				
S3 275-315	300	#7 (297.0)	#7		
					Med. chocolate
	320				
S2 315-325					
	340	#8 (339.0)	#8		Transition to dark chocolate, foram rich
S1 325-365				A (350)	
	360				
	365				Dark grey brown

CORE 15

Section	Depth cmbsf	Pore Water	Porosity	Smear Slide	General Description
	0				
		#1 (8)	#1 (13)	E (4)	
	20				
		#2 (22)	#2 (26)		
S3 (44)	40				
		#3 (54)			
	60				Medium chocolate brown matrix. Stiff. Foram Rich.
	80				
S4 (94)		#4 (85.5)	#4 (88)		
	100				
				D (114)	
	120				
	140				
		#5 (143.5)	#5 (147)		Darker chocolate brown zone. Less Stiff. Decreased forams.
	160				
	180				
S3 (194)					
	200				
	220				
				C (234)	
	240				
		#6 (241.5)	#6 (248)		
	260				
	280				Transition from dark to medium chocolate brown matrix.
S2 (294)		#7 (299.0)		B (299)	Remains less stiff. Increased foram content.
	300				Gradational change in matrix.
			#7 (306)		Becoming darker, less stiff, and decreasing foram content.
	320				
	340				Very stiff section.
	360				
		#8 (373.5)	#8 (380)	A (374)	
	380				Medium chocolate brown matrix. Stiff, clayey mud.
S1 (394)	394				Foram rich. Some darker brown bioturbation smudges.
					Core Cutter Dented. Reached Basement ?

CORE 16

Section	Depth cmbsf	Pore Water	Porosity	Smear Slide	General Description
	0				
		#1 (6.5)			
	20		#1 (15)		
		#2 (26.5)	#2 (31)		
	40				
S5 (56)					
	60				
		#3 (65.5)	#3 (72)		
	80				
S4 (106)	100	#4 (93.0)	#4 (99)	C (96)	
	120				
					Med. chocolate brown, less stiff, foram rich
	140	#5 (139.5)	#5 (144)		Darker, less stiff, less forams, clayey
	160				
	180				
S3 (206)	200				
					Med. brown and stiff
	220				
	240	#6 (235.5)	#6 (241)	B (236)	
	260				
	280				Mottled transition from dark to med. brown, stiff
S2 (306)	300				
	320				
					Stiffer and darker
	340				
		#7 (344.0)	#8 (348)		
	360				Less stiff and lighter
					✱ Slightly darker layer
	380				
		#8 (383.0)	#8 (388)	A (391)	
	400				
S1 (406)	406				Chocolate brown stiff mud, foram rich

CORE 17

Section	Depth cmbsf	Pore Water	Porosity	Smear Slide	General Description
	0				
		#1 (3.5)	#1 (12)		
	20	#2 (19.0)			
			#2 (25)	E (22)	
	40				
		#3 (50.5)	#3 (53)		
	60				
S4 (82)	80				
		#4 (94.5)	#4 (101)		
	100				
	120				
					Med. brown mud
	140				
		#5 (148.5)	#5 (153)	D (152)	Darker brown, clay rich, less stiff
	160				
S3 (182)	180				
	200				
	220				
		#6 (225.0)	#6 (230)		
	240				
	260				Med. brown, gritty, stiffer
		#7 (278.5)		C (277)	
S2 (282)	280				Dark brown clay rich, much less stiff
			#7 (285)		
	300				
					Glass fragments
	320				
				B (337)	
	340				
	360				
		#8 (372.0)	#8 (376)	A (370)	Glass fragments
S1 (382)	382				Med. brown clayey foram rich mud

CORE 18

Section	Depth cmbsf	Pore Water	Porosity	Smear Slide	General Description
	0				
		#1 (5.5)	#1 (7)		
	20	#2 (17.0)	#2 (21)	D (18)	
	40				
		#3 (52.0)			
S5 (68)	60		#3 (59)		
	80				
		#4 (90.5)			
	100		#4 (93)		
	120				
					Chocolate, more forams
	140	#5 (141.0)			
			#5 (147)		
S4 (168)	160				
					Darker, less stiff
	180	#6 (180.0)			
			#4 (186)	C (183)	
	200				
	220				
	240	#7 (237.0)			
			#7 (243)		
S3 (268)	260				
					Chocolate
	280				
					Sharp boundary, darker but stiff
	300				
	320				
		#8 (330.5)		B (328)	
	340		#8 (336)		
S2 (368)	360				
	380				
	400				Chocolate brown, foram rich, stiffer
		#9 (404.5)	#9 (410)		
	420				Darker, fewer forams, clay rich, less stiff
	440				
		#10 (444.5)	#10 (450)	A (448)	
	460				
S1 (468)	468				Chocolate brown, foram rich, not too stiff

CORE 19

Section	Depth cmbsf	Pore Water	Porosity	Smear Slide	General Description
	0			E (6)	
		#1 (11.0)	#1 (13)		
S4	20				Mottled, brown smudges
0-78		#2 (26.5)	#2 (30)		
	40				
		#3 (54.5)	#3 (58)	D (51)	
	60				
	80				
S3	100	#4 (100.5)	#4 (105)		
78-128					
	120				Chocolate, foram rich, less stiff
					Mottled
	140	#5 (143.5)	#5 (150)	C (146)	
	160				Mottled, darker, clayey, fewer forams, gooey
S2					
128-228	180				
	200				
		#6 (211.5)	#6 (215)		
	220				
				B (236)	
	240	#7 (237.0)	#7 (243)		
	260				
S1					
228-328	280				Dark to light chocolate brown, less stiff, clayey
					Mottled transition to darker, stiffer mud
	300	#8 (299.5)	#8 (305)	A (301)	
	320				
	328				Chocolate brwon clayey mud, some forams

CORE 20

Section	Depth cmbsf	Pore Water	Porosity	Smear Slide	General Description
	0				Light chocolate brown matrix.
		#1 (4.5)	#1 (9) **9ml**	F (5)	
	20	#2 (19.0)			
		#3 (38.5)	#2 (25)		
	40				35-45: darker bioturbation smudges.
			#3 (45)		
	60				
					less stiff
	80			E (80)	No colour change
		#4 (82.5)	#4 (89)		
	100				95-105: stiffer lens. foram rich.
S1 (105)					
	120				
					less stiff
	140				No colour change
		#5 (142.5)	#5 (149)		
	160				152-163: darker bioturbation smudges.
	180				
		#6 (186.5)	#6 (193)	D (185)	
	200				
S2 (205)					Consistency getting stiffer.
	220				No colour change.
	240				
		#7 (248.5)	#7 (253)		
	260				
	280				
	300				Light chocolate brown matrix. More stiff/sticky than gritty.
S3 (305)					(Smoother but stiffer consistency)
	320			C (320)	
		#8 (322.5)	#8 (328)		
	340				
	360				
	380				
	400				
S4 (405)		#9 (415.0)			gradual colour change medium to light chocolate brown
	420				
			#9 (421) **8ml**		
	440				
		#10 (446.0)	#10 (451)	B (450)	
	460				
	480				

	500				
S5 (505)					
	520				
		#11 (520.5)	#11 (524)		
	540				
		#12 (553.5)	#12 (557)	A (555)	
	560				
	570				Medium chocolate brown matrix. Gritty texture. Forams.
S6 (575)	575				Some bioturbation smudges.
					Core Cutter Dented. Reached Basement ?

CORE 21

Section	Depth cmbsf	Pore Water	Porosity	Smear Slide	General Description
	0				
		#1 (6.5)	#1 (11)	F (5)	
	20				
		#2 (22.5)	#2 (28)		
	40				
		#3 (43.5)	#3 (46)		
	60				
S6 (75)					
	80				
		#4 (90.5)	#4 (99)	E (90)	
	100				Slightly grittier
	120				
	140				
		#5 (140.5)	#5 (145)		
	160				
S5 (175)					
	180				Darker smudges
		#6 (189.5)	#6 (197)		
	200				
	220				
	240				
		#7 (257.5)			Slightly darker zone
	260				
S4 (275)			#7 (262)		
	280				
				D (290)	
	300				
	320			C (320)	
		#8 (322.5)	#8 (329)		
	340				
	360				
S3 (375)					Slight lightening trend
	380				
		#9 (384.5)	#9 (391)		
	400				
	420				
	440				
		#10 (449.5)	#10 (453)	B (450)	
	460				
S2 (475)					
	480				Slightly darker, grittier
		#11 (497.5)			

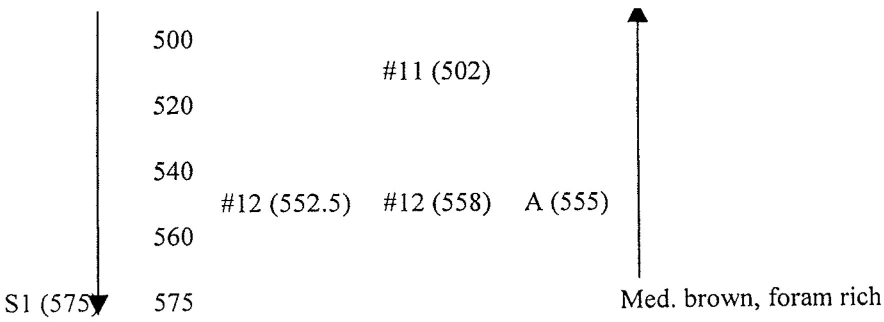
500
#11 (502)
520
540
#12 (552.5)
#12 (558)
A (555)
560
S1 (575)
575
Med. brown, foram rich

CORE 22

Section	Depth cmbsf	Pore Water	Porosity	Smear Slide	General Description
	0	#1 (4.5)	#1 (9)	E (6)	
		#2 (15.5)	#2 (22)		
	20				
S6		#3 (36.5)	#3 (43)		
0-75	40				
	60				Darker band
	80				
		#4 (90.5)	#4 (97)		
	100				
S5	120				
75-175	140	#5 (141.5)	#5 (147)	D (146)	Lighter mud
	160				
	180				
	200	#6 (191.5)	#6 (197)		
S4					Darker zone, stiff, very gritty
175-275	220				
	240				
		#7 (256.5)	#7 (262)		
	260				
					Stiffer, grittier matrix
	280			C (281)	Darker brown smudges
	300				
S3					
275-375	320	#8 (322.5)	#8 (325)		
	340				
	360				
	380				
	400	#9 (399.5)	#9 (392)	B (401)	
S2					
375-475	420				Lightening
	440				
	460	#10 (460.5)	#10 (466)		
	480				

S1	500	#11 (498.5)	#11 (504)		
475-575	520				★Darker zone
	540				
		#12 (554.5)	#12 (560)		
	560			A (561)	
	575				Med. brown, foram rich

CORE 23

Section	Depth cmbsf	Pore Water	Porosity	Smear Slide	General Description
	0				Chocolate, less stiff
		#1 (6.5)		E (5)	
	20		#1 (12)		
S19 (35)		#2 (28.0)			
S18 (45)	40		#2 (32)		Transition to lighter sediment
		#3 (46.5)			
	60		#3 (52)		
S17 (85)	80				
S16 (95)					
	100			D (100)	Darker band
		#4 (106.5)			
	120		#4 (111)		
S15 (135)					
S14 (145)	140				
					Stiffer, fewer forams
	160				
		#5 (164.5)	#5 (169)		
S13 (185)	180				
S12 (195)					
	200				
		#6 (207.5)			Med. chocolate brown, stiffer, fewer forams
	220		#6 (212)		
	240				
	260			C (260)	
		#7 (263.5)	#7 (268)		
S11 (285)	280				
S10 (295)					
	300				
	320				
	340				
		#8 (349.5)			
	360		#8 (354)		
S9 (385)	380				
S8 (395)					
	400				
	420	#9 (418.5)			Darker band, less forams, slightly gooey
S7 (435)			#9 (424)	B (430)	
S6 (445)	440				
	460				
		#10 (462.5)	#10 (467)		
S5 (485)	480				
S4 (495)					

	500			Slightly lightening
	520	#11 (513.5)	#11 (518)	
S3 (535)	540			
S2 (545)				
	560	#12 (554.5)	#12 (557)	
S1 (575)	575			A (570) Med. chocolate brown, foram rich

CORE 24

Section	Depth cmbsf	Pore Water	Porosity	Smear Slide	General Description
	0				Light brown
		#1 (2.5)	#1 (7)		
	20	#2 (14.5)			Slightly darker zone
			#2 (24)		
	40				
		#3 (42.5)	#3 (47)		
	60				
S6 (75)					
	80				
		#4 (82.5)	#4 (91)		
	100				
	120				
		#5 (133.5)	#5 (139)		
	140				
	160				Slightly darker zone
S5 (175)					
	180				
		#6 (186.5)	#6 (191)		
	200				
	220				
					Slightly darker zone
	240				
		#7 (256.5)			
	260				
S4 (275)			#7 (263)		Less gritty
	280				
	300				
		#8 (318.5)			
	320				
			#8 (326)		
	340				
	360				
S3 (375)					Light brown, foram rich, gritty
	380				
		#9 (387.5)	#9 (397)		
	400				
	420				
	440				Lightening
	460				
S2 (475)		#10 (462.5)	#10 (467)		
	480				

	500			Transition to darker chocolate brown
		#11 (502.5)	#11 (507)	↑
	520			
	540			
		#12 (545.5)	#12 (551)	
	560			
S1 (575) ↓	575			Brown, foram rich, stiff mud

CORE 25

Section	Depth cmbsf	Pore Water	Porosity	Smear Slide	General Description
	0			F (1)	
		#1 (5.5)	#1 (10)		
	20				24: Light chocolate mud to top
		#2 (25.5)	#2 (29)		
S19 (34)	40				
S18 (44)					Transition to darker mud. Bioturbation. Mottled with
	60	#3 (51.5)	#3 (57)		dark and medium brown mud.
					64-87: Graded bed of foram sand. Some basalt
	80			E (74)	fragments. Tan-Khaki mud.
S17 (84)					101-87: darker brown zone
S16 (94)	100				
	120	#4 (118.5)			
			#4 (122)		
S15 (134)	140				
S14 (144)					Stiff light chocolate brown mud
	160				
		#5 (164.5)	#5 (170)		
	180				
S13 (184)					
S12 (194)	200				
		#6 (202.5)	#6 (208)	D (204)	
	220				Light chocolate brown mud
					220-229: Graded bed of forams and basalt fragments.
	240				
	260				
		#7 (261.5)	#7 (266)		
	280				
S11 (284)					
S10 (294)	300				
					314: Transition to light chocolate brown matrix.
	320				Less stiff in consistency.
				C (329)	
	340	#8 (333.5)	#8 (336)		
					344-354: Highly bioturbated. Darker brown matrix.
	360				
	380				Lightening from darker brown to chocolate brown.
S9 (384)					Still stiff consistency.
S8 (394)	400				
					403-405: Foram sand layer. Tan-Khaki coloured matrix.
	420	#9 (413.5)	#9 (418)	B (414)	
					Transition to darker brown from chocolate to medium brown.
S7 (434)	440				
S6 (444)					
	460				
		#10 (460.5)	#10 (465)		
	480				Slightly darkening to chocolate brown. Remains stiff
S5 (484)					Increasing evidence of bioturbation

S4 (494)	500				
	520	#11 (512.5)	#11 (517)		
S3 (534)	540				
S2 (544)					
	560	#12 (552.5)	#12 (557)	A (554)	
	570				
S1 (574)	574				Fine light chocolate brown. Low foram content. Stiff mud.

CORE 26

Section	Depth cmbsf	Pore Water	Porosity	Smear Slide	General Description
	0			C (2)	
		#1 (30.5)	#1 (38)		
	20				(basalt fragment)
	40				
		#2 (57.5)	#2 (56)		
S1	60				Light tan brown, more forams, less stiff
0-150		#3 (71.5)	#3 (79)		
	80				Bioturbated, darker zone
		#4 (90.5)	#4 (95)	B (90)	
	100				
		#5 (116.5)	#5 (108)		
	120				Increasing bioturbation and forams
	140	#6 (143.5)	#6 (135)	A (144)	(basalt fragment)
	150				Light- tan brown, stiff, low in forams

CORE 27

Section	Depth cmbsf	Pore Water	Porosity	Smear Slide	General Description
	0				Light brown, squishy, foram rich
		#1 (7.0)	#1 (12)		
	20				Darker brown, lightening
		#2 (23.5)	#2 (28)	F (23)	???
S19 (35)	40				
S18 (45)		#3 (52.0)	#3 (56)		
	60				Darker zone
		#4 (64.0)	#4 (69)		
	80				
S17 (85)					
S16 (95)	100				
		#5 (113.5)	#5 (118)		
	120				
				E (133)	Lightening in colour, increasing forams
S15 (135)	140				
S14 (145)					
	160				
	180				
					Light brown
	200				Transition from chocolate to light brown
		#6 (205.5)	#6 (211)		
	220				
				D (228)	
S13 (235)	240				
S12 (245)					
	260				Chocolate brown
					Transition from light to chocolate brown
	280				
		#7 (288.5)	#7 (295)		
	300				Increasing bioturbation
				C (308)	
	320				
					Layer of forams and glass fragments
S11 (335)	340				
S10 (345)					
	360				
		#8 (362.5)	#8 (369)		
	380				
S9 (385)					
S8 (395)	400				
		#9 (418.5)			
	420		#9 (421)		
S7 (435)	440				
S6 (445)					
	460				Light brown
		#10 (467.5)	#10 (471)		Transition to light brown
	480				
S5 (485)				B (483)	

S4 (495)	500				
		#11 (517.5)	#11 (519)		
	520				
S3 (535)	540				
S2 (545)		#12 (554.5)			
	560		#12 (560)		
				A (573)	
S1 (575)	575				Dark chocolate brown, few forams

CORE 28

Section	Depth cmbsf	Pore Water	Porosity	Smear Slide	General Description
	0				Gooey light brown
				F (5)	Forsm rich sandy layer
	20		#1 (19)		Forsm rich sandy layer
		#1 (27.5)			Light brown
	40	#2 (38.5)	#2 (32)		Forsm rich sandy layer
	60				
		#3 (61.0)	#3 (64)		
S6 (75)	80	#4 (78.5)			Med. tro light brown
			#4 (85)	E (85)	Forsm rich sandy layer
	100				
	120				
					Light- med. brown
	140	#5 (132.5)			Forsm rich sandy layer
			#5 (141)		
	160				
					Darkening to light brown
S5 (175)	180				
		#6 (186.5)		D (190)	
	200		#6 (192)		
					Lightening to tan
	220				
	240				
					Graded foram and basalt sand
	260				
		#7 (269.5)	#7 (262)		
S4 (275)	280				
	300				Coarse foram and balast sand
				C (305)	
	320				
	340	#8 (334.5)	#8 (338)		
	360				
S3 (375)	380				
	400	#9 (393.5)	#9 (399)		
	420				Light brown
	440				
	460	#10 (456.5)		B (455)	
			#10 (461)		
S2 (475)	480				Foram rich layer with some glass fragments

	500				
	520				
		#11 (525.5)	#11 (528)		
	540				
	560	#12 (554.5)	#12 (560)	A (555)	
S1 (575)	575				Medium brown, stiff, some forams, bioturbated

CORE 29

Section	Depth cmbsf	Pore Water	Porosity	Smear Slide	General Description
	0				
				F (5)	
	20	#1 (15)			Medium brown, soupier, more forams
			#1 (21)		
S19 (25)	40				
S18 (35)		#2 (40.5)	#2 (44)		
	60	#3 (53.5)	#3 (59)		
		#4 (67.5)	#4 (73)		
S17 (75)	80				
S16 (85)					
	100				
		#5 (105.5)	#5 (110)	E (105)	
	120				
S15 (125)					Increasing forams
S14 (135)	140				
	160	#6 (154.0)	#6 (156)		
S13 (175)	180				
S12 (185)					
	200				
	220				
		#7 (222.5)	#7 (226)		
	240				
				D (250)	Dark brown, low forams, clayey, less stiff
	260				
					Gradual transition to dark brown
S11 (275)	280				
S10 (285)					
	300				
	320			C (320)	
		#8 (321.5)	#8 (327)		
	340				
	360				
S9 (375)	380				
S8 (385)					
	400				
		#9 (402.0)	# 9(407)	B (405)	
	420				
S7 (425)					Increasing bioturbation
S6 (435)	440				
	460	#10 (453.0)	#10 (457)		
S5 (475)	480				
S4 (485)					

	500				
		#11 (500.5)	#11 (503)		
	520				
S3 (525)					
S2 (535)	540				Transition to lighter tan-khaki
		#12 (543.5)	#12 (546)	A (545)	Slight darkening
	560				
S1 (565)	565				Stiff tan-khaki, low forams, clayey

CORE 30

Section	Depth cmbsf	Pore Water	Porosity	Smear Slide	General Description
	0				Bent barrel, top portion of core lost!
				E (2)	
S19 (20)	20	#1 (10.5)	#1		
S18 (30)					
	40				
		#2 (50.0)	#2		
	60				
S17 (70)					
S16 (80)	80				
				D (90)	
	100				
		#3 (101.5)	#3		
S15 (120)	120				
S14 (130)					
	140				
	160	#4 (151.5)	#4		
S13 (170)					
S12 (180)	180				
	200				
	220				
	240	#5 (234.0)	#5	C (235)	
	260				Fudge brownie, less stiff
S11 (270)					Highly mottled transition to dark brown
S10 (280)	280				
	300				
S9 (320)	320				
S8 (330)					
	340				Increasing bioturbation
		#6 (347.0)	#6	B (350)	
	360				
S7 (370)					
S6 (380)	380				
	400	#7 (399.0)			
			#7 (403)		
S5 (420)	420				Slightly lighter tan-khaki
S4 (430)					
	440				
	460	#8 (450.5)	#8 (456)		
S3 (470)					
S2 (480)	480				
				A (490)	

500

S1 (510) ▼ 510 Dark tan-khaki, clayey. Low forams, stiff